MODIFICATIONS TO THE RESEARCH WSR-88D
TO OBTAIN POLARIMETRIC DATA

R. J. Doviak
J. Carter
V. Melnikov
D. S. Zrnic

National Severe Storms Laboratory
1313 Halley Circle
Norman, Oklahoma 73069

May 1, 2002

MODIFICATIONS TO THE RESEARCH WSR-88D
TO OBTAIN POLARIMETRIC DATA

TABLE OF CONTENTS

MODIFICATIONS TO THE RESEARCH WSR-88D
TO OBTAIN POLARIMETRIC DATA

PREFACE

This report describes the modifications made to the National Severe Storms Laboratory's (NSSL) research and development WSR-88D to provide polarimetric capability. The radar has the following two options: (1) to simultaneously transmit horizontally (H) and vertically (V) polarized pulses, and simultaneously receive and process the H and V echoes, and (2) to transmit only horizontally polarized signals, as is presently available with the WSR-88D operational radars, but to receive both co-polar and cross-polar polar echoes to derive other polarimetric variables (e.g., linear depolarization ratio, etc.). In addition to providing research data to NSSL and other scientists, the R&D WSR-88D serves as a test bed radar to evaluate possible upgrades to the network of WSR-88Ds operated by the NWS.

This report is divided into two parts; the first describes the changes made to the microwave hardware to obtain transmission and reception of horizontally and vertically polarized signals, and the second part describes the installation of a second WSR-88D receiver for the V channel and an interface (i.e., the Dual-Pol Frequency Generator) that allows integration of a commercial off-the-shelf processor (i.e., SIGMET's RVP7/IFD) into the radar without impacting the performance of the existing receiver/processor (i.e., the two receivers and processors run concurrently).

The final configuration of the receiver for processing the two orthogonally polarized signals has not yet been established. The current implementation is a proof of concept and includes the SIGMET's RVP7/IFD processor. That processor does not support many of the WSR-88D operating modes and contains proprietary details which would preclude its direct inclusion into the open RDA. Nevertheless, the processor has the capability to deliver the polarimetric variables with a relatively modest amount of engineering changes, and as well, incorporates a digital receiver. Digital receivers are presently being evaluated as candidates to replace the WSR-88D's analog receivers which are rapidly becoming outdated.

Hardware changes to the antenna involving the installation of a dual polarized feed, and the performance of the modified antenna, is described by Doviak et al., (1998). In short, the new dual polarized feed generates radiation patterns that meet present specifications of the WSR-88D for horizontally polarized transmissions, and, as well, can provide vertically polarized transmissions that have radiation patterns matched to those of the horizontally polarized waves. If the NWS decides to implement the dual polarized mode on its network of WSR-88D radars, the microwave hardware modifications made to NSSL's R&D WSR-88D (mostly additional WSR-88D components) could be replicated, with minor changes, on the operational WSR-88D radars.

On the other hand, the processor (i.e., SIGMET's RVP7/IFD) currently passively connected to the R&D WSR-88D to provide polarimetric data and possibly test proposed engineering changes to the WSR-88D (e.g., to mitigate range velocity ambiguities), does not meet many of the specifications of the WSR-88D. Thus the processors that will be integrated into the operational network of radars could be very different. Nevertheless, SIGMET's RVP7/IFD has the capability to process dual polarized signals and provide the research community a WSR-88D polarimetric radar for experimentation, and evaluation of meteorological products that can be generated by the polarimetric radar.

PART I: MODIFICATIONS TO THE WSR-88D MICROWAVE HARDWARE AND MEASUREMENTS OF ITS PERFORMANCE

1.1 INTRODUCTION

The hardware modifications to the R&D WSR-88D that are described in this section have been made by NSSL engineers using commercial off-the-shelf microwave components (mostly WSR-88D spare parts). Some of these microwave components and waveguides are mounted on an aluminum frame, and were assembled in a laboratory where measurements were made to determine insertion losses between various ports. This entire assembly has been moved to the base of the antenna pedestal in the radome atop the WSR-88D tower (Fig.1.1). In the Spring of 2001, this assembly was connected to a specially designed dual channel azimuth rotary joint leading to two single channel elevation rotary joints (one for H and one for V).

1.2 THE LAYOUT OF MICROWAVE COMPONENTS IN THE RADOME

a) *Loss factors if both H and V channels are energized*

Fig. 1.2 is the block diagram of the principal microwave components housed in the radome. These are used to (1) transmit linearly polarized H-waves as presently done in the WSR-88Ds, but to receive both H and V, the copolar and cross-polar weather echoes, or (2) transmit elliptically polarized waves with equal H and V amplitudes and receive simultaneously the H, V polarized weather echoes. Figure 1.1 shows some of the components in the block diagram of Fig.1.2. The center gray-colored waveguide exiting the hatch at the base of the pedestal in Fig. 1.1(a), and connecting to the white colored guide, carries the transmitted power to switches SW1, SW2. On either side of this white-colored guide are two beige- colored waveguide components; these are the circulators. Ports 2 of these circulators, which feed transmitted power to the antenna, are on the right side (connected to the blue colored guides), and ports 3 on the left side of the circulators deliver the echo power to the Receiver Protectors and Low Noise Amplifiers (LNAs) located behind the waveguide filters (the gray-colored guides with 15 tuning screws).

The simultaneous reception of H, V echoes when only H is transmitted will allow measurement of the Linear Depolarization Ratio LDR_{vh} (the first subscript denotes the received polarization and the second the transmitted polarization; Doviak and Zrnic, 1993, Section 8.5.2), and the magnitude and phase of the copolar to cross-polar correlation coefficient. The simultaneous reception with simultaneous transmission of H, V waves will provide the copolar correlation coefficient, differential phase, and differential reflectivity. In both modes, the spectral moments (reflectivity, Doppler velocity, and spectrum width), presently available from the WSR-88D, will continue to be provided with the same levels of accuracy.

3

The wave guide switches SW1 and SW2 determine whether the radar operates in a linearly polarized mode (i.e. to transmit only H-waves), or in the dual H, V mode (both H and V polarized waves are transmitted simultaneously). In Fig. 1.2, the switches are in the de-energized position, and the system simultaneously transmits and receives H, V signals. The encircled numbers refer to the ports used in the measurement of insertion losses; the numbers next to some components label the ports of that device. The dual channel azimuthal rotary joint, plus mating dual channel waveguide assemblies inside the pedestal housing, were manufactured by Diamond Antenna & Microwave Corp.; their specifications are given in Appendix 1. Most all of the other devices with the exception of the magic-tee power-splitter shown in Fig. 1.2 are standard components for WSR-88D. Detailed descriptions of these can be found in the WSR-88D field manuals that are cataloged by the Radar Operations Center in Norman, OK.

Table 1.1 gives the loss factors L(m, n) between the various "measurement" ports identified by circled numbers in Fig. 1.2; the first index defines the output port and the second the input port. These measurements were made before the assembly was connected to the dual channel azimuth rotary joint and the WSR-88D's receiver. Loss factors from measurement ports 1 to 2, $L(2,1) = 3.4$ dB, and from ports 1 to 3, $L(3,1) = 3.3$ dB, are for the most part (i.e., 3 dB) due to the transmit power-splitter (Fig. 1.2) which is a magic tee (Keflas and Wiltse, 1970). The magic tee splits the power that is incident on its device port 1 (indicated by small numerical numbers on the periphery of the device) into device ports 2 and 3. Device ports 1, 2, and 3 are so-called H-plane ports, and any reflection from the circulators is split between device ports 1 and 4, and reflected power from the V circulator does not emerge from device port 2, and reflections from the H circulator does not emerge from device port 3. That is, device ports 2 and 3 are isolated.

From these measurements, it can be inferred that the transmit propagation path losses due to mismatch at device interfaces and waveguide bends, and absorption through the waveguides *and circulators*, are less than 0.4 dB, and are about equal. From the input of switch SW1 to the azimuth rotary joint, the transmitter path loss for the H and V channels are within 0.1 dB of one another.

Table 1.1: Loss factors (dB) between ports in the H, V dual mode

$L(2, 1) = 3.4$ dB	$L(1, 3) = 28.5$ dB	$L(2, 3) = 49.9$ dB	$L(4a, 2) = 1.4$ dB
$L(3, 1) = 3.3$ dB	$L(1, 2) = 30.5$ dB	$L(3, 2) = 51.9$ dB	$L(4a, 3) > 70$ dB

The loss factors from measurement ports 3 to 1, and from 2 to 1 (i.e., losses in the reverse direction, $L(1, 3) = 28.6$ dB and $L(1, 2) = 30.5$ dB; Table 1.1), are principally due to the loss factor between the circulators' device ports 2 and 1, but includes a 3 dB loss through the magic-tee power-splitter. Thus, ignoring losses in waveguides and mismatch losses at device interfaces, the loss between the device ports 2 and 1 of the H circulator is about 27.5 dB whereas the equivalent loss in the V circulator is about 25.6 dB, a 1.9 dB difference. Nevertheless, these

4

relatively large loss factors show that a negligible fraction of the echo powers entering the receiver chains at Port 2 of the circulators is coupled to the transmitter line. Any power that is reflected back to the transmitter passes to a circulator above the transmitter cabinet where it dissipates in a termination. The circulator in the transmitter building serves the purpose to isolate the transmitter tube from reflected powers.

The loss factors from measurement ports 2 or 3 (i.e., the inputs are to the circulator ports 2) to measurement ports 3 or 2 (i.e., $L(3, 2) = 51.9$ dB, $L(2, 3) = 49.9$ dB; Table 1.1) is due to the isolation provided by the magic-tee power-splitter and the isolation losses in the circulators when signals are propagating in a direction opposite to the normal power flow direction (indicated by the arrows on the sketches of the circulators). During these measurements, the azimuthal rotary joint was not connected. As pointed out in a previous paragraph, the magic tee has the ideal property that its ports 2 and 3 are isolated. Although the measurements show significant loss (i.e., 49.9 and 51.9 dB), ideally the loss factor between these ports should be infinite. Using the estimate of the loss factor in each of the circulators (i.e., 25.6 and 27.5 dB), the isolation provided by the magic tee is computed to be about 24.4 dB for transmissions from device ports 2 to 3 of the magic tee, and is *exactly the same*, as expected, for transmissions from device ports 3 to 2. The magic tee isolation agrees well with the manufacturer's (Microwave Development Laboratories, Inc) specification that the isolation for collinear arms (i.e., device ports 2 and 3) is >20 dB. The isolation between device ports 1 and 4, although not measured, is specified to be larger than 30 dB.

The high loss factors in the magic tee and the circulators should keep the two receivers relatively isolated from each other. But the above measurements do not account for additional coupling between the channels when the rotary joints and antenna feed are connected. For example, before the assembly was interfaced with the WSR-88D radar, measurements of insertion loss between ports 4a and 3 show isolation larger than 70 dB (i.e., Table 1.1, $L(4a, 3) > 70$ dB).

But of importance, after the rotary joints and antenna feed were connected, is the coupling of power that is received in the H antenna port 6 and appears in the V channel output at port 5 (i.e., $L(5, 6)$, and vice versa (i.e., $L(4, 7)$). Measurements when power was inserted into port 6 (i.e., the H antenna port) and measured at the H and V output ports 4 and 5 show that the cross-coupled power is about 50 dB below the co-coupled power (i.e., $L(5, 6) \approx L(4, 6) + 50$ dB). Furthermore, when power is inserted into port 7, the ratio of powers in ports 4 and 5 is about 58 dB (i.e., $L(4, 7) \approx L(5, 7) + 58$ dB). Note that the loss factors $L(4, 6)$ and $L(5, 7)$ are negative because the gain of the low noise amplifiers (LNAs; Fig. 1.2) overcomes the losses in their respective paths.

The cited loss factors assume that the cross-coupled power passes through the LNA circuits. It is not known what path the cross-coupling takes, but the fact that there is a difference (i.e., 50 vs. 58 dB) in the two measurements suggest that the circulators might be contributing, or that the radiation is coupled after passing through the antenna feed to the outside. Some of the

5

coupling comes through the dual channel azimuth rotary joint. The specified isolation of this rotary joint is that it be larger than 50 dB, and these measurements confirm that this condition is satisfied. The fact that the cross-coupled power is more than 50 dB below the co-coupled power means that Linear Depolarization Ratio LDR measurements will not be compromised by cross-coupling in the microwave circuits. The cross- coupling between H and V in the radiation emitted by the antenna is about 32 dB (Doviak et al., 1998), and thus the antenna coupling limits the smallest LDR that is measurable.

The data in Table 1.1 shows that the loss factor L(4a, 2) along the receiver path from the horizontal channel's circulator input at Port 2 (also the device port) to the receiver protector output at Port 4a is 1.4 dB. Measurements were not made of L(5a, 3), but its value should be similar to L(4a, 2). These are significant losses that decrease the echo power and increase the noise power N and, consequently, decrease the Signal-to-Noise Ratio, *SNR,* of weather echoes. But there is little that can be done about this without major changes in the system; furthermore, these losses are inherently a part of the WSR-88D design. Nevertheless, for most weather observations, the *SNR* is more than adequate.

Note that L(4a, 2), if computed from the sum of the loss factors for each of the components in Fig. 1.2, calculates to be about 2.4 dB, assuming that the circulator's loss factor between device ports 2 and 3 is at most 0.2 dB. The value of 0.2 dB is the measured loss, reported in Table 1.2 of section 1.2(e), between the measurement ports 1 and 2 when switch SW1 is set so that only H power is transmitted; this switch position removes the magic tee from the circuit. Ignoring waveguide losses, the measure 0.2 dB loss factor is the forward loss between the circulator's ports 1 and 2, and it is assumed to be equal to the forward loss between the circulator's ports 2 and 3. Although the calculated 2.4 dB value differs significantly from that 1.4 dB measurement reported in Table 1.1, calibration of the radar will resolve any differences, and also provide the means to obtain correct estimates of echo power at Port 2a, the calibration port. Loss factors, not in the calibration path (e.g., the circulators and rotary joints, antenna gain) however, need to be carefully evaluated periodically to insure the radar is correctly calibrated.

b) *Measurements of transmitted powers*

The transmitted H and V powers are monitored with power meters at ports 6 and 7 which are designated as the "antenna ports". Measurements of transmitted powers in the dual transmit mode and the single H transmit mode show the following results:

Dual H, V mode:
      160 kW peak at port 6 (H antenna port)
      143 kW peak at port 7 (V antenna port)

H mode:

 323 kW peak at port 6

 < 1 watt peak at port 7

Based upon insertion loss measurements $L(2, 1)$ and $L(3, 1)$ reported in Table 1.1, and the specified 0.1 dB larger power loss in the vertical channel of the azimuth rotary joint, it was expected that the H and V powers would be nearly the same. However, the above measurements show that the H power at the antenna port is about 0.5 dB higher than the V power. But loss factor measurements were made several months before the components in Fig. 1.1(a) were installed in the radome. Thus, the loss measurements reported in Table 1.1 do not include the additional losses associated with the various waveguide components (i.e., flexible guides, bends, etc.) required to interface the components shown in Fig. 1.1(a) to the dual channel azimuth rotary joint and the transmitter. Furthermore, the vertical channel has three flexible waveguides (two above the elevation housing) whereas the horizontal channel has one (see Figs. 1.1a and A1.4). The additional flexible waveguides could account for the 0.5 dB lower transmitted power in the vertical channel.

To support this interpretation, loss factors, $L(3a, 7)$ and $L(2a, 6)$ of the V and H channels were measured in the Fall of 2001 after the microwave components were interfaced with the radar as shown in Fig. 1.1(a). These measurements showed that loss factors $L(2a, 6)$ and $L(3a, 7)$ are 1.2 dB and 0.65 dB respectively. These losses include those in the rotary joints, circulators, waveguide bends, and flexible guides. Measurements of $L(3a, 7)$ have an uncertainty of about ± 0.2 dB based upon uncertainties in the coupling factor ($C_7 = 44.3 \pm 0.2$ dB) of the directional coupler at port 7. Thus, it is likely that the 0.5 dB larger H transmitted power is due to the 0.55 dB smaller attenuation in the waveguide circuits from the H circulator to port 6. Monitoring of the transmitted powers should verify whether the 0.5 dB difference is a bias in the loss factors that needs to be corrected or accounted for in routine calibrations.

The peak power levels of the transmitter at the waveguide switch 1S1 in the transmitter building was about 710 kW. Thus the following loss factors, from the 1S1 switch to the antenna ports, are computed:

$$L(6, 1S1) = 6.47 \text{ dB (H, V mode)}$$
$$L(7, 1S1) = 6.96 \text{ dB (H, V mode)}$$
$$L(6, 1S1) = 3.42 \text{ dB \quad (H mode)}.$$

$L(6, 1S1) = 3.42$ dB is significantly more than what would be expected (≈ 0.8 dB) from the approximately 25 m of aluminum waveguide that connected the 1S1 switch in the transmitter building to the circulator when it was in the base of the antenna pedestal. The 0.8 dB is the calculated loss before the dual channel modifications were made to the radar. Considering that there is less than a 0.1 dB loss in the H channel of the new azimuth rotary joint, a less than a 0.05 dB loss in the elevation rotary joint, and a measured 0.2 dB loss in the H circulator (Table I.2; $L(2, 1)$), the loss factor from 1S1 to the circulator input port 1 for the modified radar calculates

(3.42 - 0.35) to about 3 dB. This is more than 2 dB larger than that calculated for the original single channel WSR-88D. This added insertion loss is likely due to the numerous waveguide bends and flexible waveguides needed to join the various components using standard fittings. For example, see the numerous bends and flexible guides entering the base of the pedestal on the right side of Fig. 1.1(a).

c) *Antenna gain*

Ports 6 and 7 are the closest and most convenient to the antenna feed's H and V ports, and that is where the antenna's H and V gains, g_H and g_V, are usually measured. Measurement ports 6 and 7 are therefore called antenna ports. This is where the transmitted powers are also measured. But, because the calibration signals are injected into cross- guide couplers at ports 2a and 3a, the received signal powers and noise powers are monitored at ports 2a, and 3a. Furthermore, measurements of the sun's radiation, to monitor the antenna gain and receiver calibration, is referenced to ports 2a and 3a. To obtain antenna gain from measurements of the sun's radiation power, the losses from antenna ports 6 and 7 to ports 2a and 3a need to be taken into account. These are repeated here for convenience:

$L(2a, 6) = 0.65$ dB
$L(3a, 7) = 1.2 \pm 0.2$ dB

The adaptation table for the R&D WSR-88D gives the antenna gain, $G_H = 10 \log(g_h) = 43.3$ dB. This H channel gain value differs considerably from that (i.e., $\approx 45.3 \pm 0.1$ dB) provided by Pratt and Ferraro (1995; Fig. 9) for this WSR-88D operating at the frequency of 2905 MHz. They show antenna gain, G_H, including radome loss, to lie between 45.2 and 45.4 dB, depending on which of four cited references are used. Because the adaptation table datum is updated with sun scans, the 43.3 dB entry is likely the antenna gain at the calibration port. In that case, the loss factor $L(2a,6) = 0.65$ dB needs to be added to the measured antenna gain entry in the adaptation table to obtain the H channel antenna gain referenced to the antenna port.

Assuming that the measured adaptation parameter for antenna gain is referenced to the H calibration port, we add $L(2a, 6) = 0.65$ dB to 43.3 dB to obtain a measured gain, referenced to the antenna port, of about 44 dB for the H polarized transmission. This still underestimates by more than a dB the theoretical data presented by Pratt and Ferraro (1995). On the other hand, Skolnik (2001, p541) suggests that the formula

$$g \approx \frac{26,000}{\theta_1^2}$$

gives a better approximation for gain, where θ_1 (in degrees) is the one-way three dB width of the H channel radiation pattern. This gain, however, does not consider the radome loss. The insertion loss of the radome, when dry, is about 0.15 dB (Pratt and Ferraro, 1995), and this value needs to

be subtracted from gain (in dB) computed from the above formula. Thus the H channel gain (in dB) obtained from the above formula, corrected for radome loss, is:

$$G_H = 44.15 - 0.15 - 20\log_{10} \theta_{1_h}$$

The one-way H channel beam width, after the dual polarized feed was installed on the antenna, is $\theta_{1_h} = 0.93°$ (this is nearly equal to the V channel beam width of 0.90°: Doviak et al.,1998). Using this θ_{1_h} value in the above formula, and accounting for radome loss, the theoretical antenna gain (in dB) computes to be about 44.63 dB, about 0.7 dB more than that computed (i.e., 43.95 dB) using the measured gain value (i.e., 43.3 dB) from the adaptation table, but referencing this gain to the antenna port 6 by adding the loss factor $L(2a,6)$. Sun calibrations can determine whether the 0.7 dB difference is a bias, or is part of statistical variations that might be expected from sun calibrations (Pratt and Ferraro, 1995). If it is a bias, the source of the bias should to be found, so that the correct antenna gain is used in the weather radar equation.

d) *Referencing echo power measurements to the antenna port*

Echo power measurements are always made at the output of the receivers (typically in digital format at the output of the signal processor), but are usually referenced to the antenna port. This is also the port where the transmitted power is measured in the WSR-88D, and as a result this can be the common reference port for the echo, noise, and transmitted power measurements. But the system gain, g_s, from the antenna port to the receivers' output, where the power is measured, is needed. The system gain can be obtained by measuring the gain from the calibration ports at the cross guide couplers (Fig. 1.2), and adding the loss factors $L(2a, 6)$, or $L(3a, 7)$. The mean weather signal power $\bar{P}(r_o)$ at the receivers' output can be related to the reflectivity factor Z of liquid precipitation at range r_o using the radar equation (Doviak and Zrnic, 1993, Eq.4.34)

$$\bar{P}(r_o) = \frac{\pi^3 P_t g^2 g_s \theta_1^2 c\tau |K_w|^2 Z}{2^{10}(\ln 2)\lambda^2 r_o^2 l^2 l_r}$$

in which all units are MKS. This equation applies to both the H and V echo powers, but parameters P_t, g, g_s, θ_1, and Z all could be different for the H and V polarized signals. Losses of power through the radome, in the antenna's reflector and feed, as well as the losses in the waveguides from the feed to the antenna port are contained in the one-way antenna gain, g, referenced to ports 6 or 7, for the H or V channels. P_t is the transmitted peak power measured at the antenna port; θ_1 is the one-way beamwidth in radians (1.62×10^{-2} for the H channel, and 1.57×10^{-2} for the V channel); c the speed of light; τ the transmitted pulse width; $|K_w|^2 = 0.93$ is obtained from the complex refractive index K_w of water (Doviak and Zrnic, 1993, Section 3.2); λ is the radar wavelength; l is the one-way loss factor (i.e., a number larger than one) due to attenuation of the signals along the atmospheric propagation path; and l_r is the loss factor due to

the finite bandwidth of the receiver (op. cit., Section 4.4). Parameters P_t, g_s, and g in the above equation (e.g., gains) must be referenced to a common port (e.g., the antenna port).

Likewise the noise power, measured at the cross- guide couplers (i.e., the calibration port), is often referenced to the antenna port. For example, the specified noise level for the WSR-88D at the antenna port is -113 dBm (Doviak and Zrnic, 1993, Table 3.1). Noise power N and SNR are required for censoring data that are not reliable. However, the calculation of noise power at the antenna port, using the noise power measured at the calibration port where the cross- guide coupler is located (Fig. 1.2), is not as simple as that required to calculate the system gain from the antenna port. Because the components add noise power, one cannot simply decrease the noise power by the loss factors L(3a, 7) or L(2a, 6). For example, if the noise power $N(2a)$ is calculated from calibration, it is related to the noise power $N(6)$ at antenna port 6 by the following equation (Doviak and Zrnic, 1993, section 3.51)

$$N(2a) = \frac{N(6)}{\ell_{2a,6}} + kT_A B_n \left(1 - \frac{1}{\ell_{2a,6}} \right)$$

where $\ell_{2a,6}$ is the loss factor, $\ell_{2a,6} = 10^{L(2a,6)/10}$, of the components which have loss $L(2a,6)$, the second term is the noise power contributed by those components, T_A is their ambient temperature in degrees Kelvin, $k = 1.38 \times 10^{-23}$ W·s·K^{-1} is the Boltzmann constant, and B_n is the noise bandwidth ($B_n = 0.63$ MHz for the short transmitted pulse mode used in storm data collection; Doviak and Zrnic, 1993, Table 3.1).

e) *Loss factors if only the H channel is energized*

The schematic in Fig. 1.3 describes the microwave layout when the switches are energized so that only horizontally polarized waves are transmitted. In this case the power-splitter magic-tee is bypassed and the large loss factor L(3, 1) > 70 dB listed in Table 1.2 is principally due to the isolation imposed by Switch SW1. The decrease of $L(2, 1)$ from 3.4 dB (Table 1.1) to 0.2 dB (Table 1.2) is principally due to the fact the power splitter is bypassed in the H-only mode. The added 0.2 dB decrease in loss is likely that due to losses in the power splitter, a loss equal to that specified by the manufacturer. Likewise we should expect that the circulator's reverse loss factor (i.e., for propagation in a direction opposite to the normal flow of power as indicated by arrows on the circulators drawn in Fig. 1.3) $L(1, 2) = 28.5$ dB to be about 3 dB less in the H alone mode than in the dual mode (i.e., dual mode $L(1, 2) = 30.5$; Table 1.1) because the power-splitter is bypassed. But the reverse loss factor in the circulator for the H-only mode is 1 dB higher than for the dual mode; the cause of this 1 dB difference is not understood, but might be related to the small changes in impedance presented to the circulators ports for the two waveguide switch positions.

10

Table 1.2: Loss factors (dB) between ports in the H-only mode

$L(2, 1) = 0.2$ dB	$L(1, 3) > 70$ dB	$L(2, 3) > 70$ dB	$L(4a, 2) = 1.3$ dB
$L(3, 1) > 70$ dB	$L(1, 2) = 28.5$ dB	$L(3, 2) > 70$ dB	$L(4a, 3) > 70$ dB

The larger than 70 dB loss factors for L(2, 3), L(3, 2), L(3, 1), and L(4a, 3) are principally due to the fact that the power-splitter is removed from the circuit when the switches are set to transmit H alone. The 0.2 dB loss factor for L(2, 1) is mostly in the H circulator from device ports 1 to 2 because attenuation in the aluminum guides, connecting the circulator to the switches, is about 0.03 dB per meter, and guide lengths are less than a meter.

L(4a, 2) = 1.3 dB (Table 1.2) for the single H polarized signal transmission is in reasonable agreement with L(4a, 2) = 1.4 dB (Table 1.1) for dual H, V transmissions; ideally they should be the same. But it is unlikely that our measurements have an accuracy better than about 0.1 Db.

Another loss factor of interest is L(4a, 1) = 23.23 dB. This is principally the loss factor between device ports 1 and 3 of the H channel circulator. This loss factor was measured when device port 2 was terminated. If the input impedance to the waveguides connecting device port 2 to the azimuth rotary joint is equal to that for the termination, then L(4a, 1) = 23.23 dB should also be the expected isolation between the transmitter and receiver when the microwave components are connected to the rotary joints in the antenna pedestal as shown in Fig. 1.1(a). This loss factor determines the amount of transmitted power that is coupled to the receiver. Thus, considering that about 300 kW of peak power is incident on device port 1, about 1.4 kW of peak power is incident on the receiver chain. But this large power is further attenuated by the action of the receiver protector and limiter (Fig. 1.3), so that significantly less power is incident on the low noise amplifier (LNA).

The experimental configuration in Figs. 1.2, 1.3 will be evaluated for practical utility and cost effectiveness. The two modes of operation can be used sequentially from volume scan to volume scan. That is, volume scans with simultaneous transmission and single polarization transmission modes could alternate; if further research proves that the cross-polar signals are important that could be a viable strategy. Note that the cross-polar signals can provide good discrimination between rain and snow (Zrnic, et al., 2001. In case that the cross-polar signals are deemed of marginal value, the system configuration can be simplified by omitting the mechanical switches.

PART II: IMPLEMENTATION AND DESCRIPTION OF A RECEIVER TO SIMULTANEOUSLY PROCESS HORIZONTALLY AND VERTICALLY POLARIZED WEATHER SIGNALS

2.1 INTRODUCTION

In parallel to the present WSR-88D analog receiver, NSSL has interfaced a single digital receiver (i.e., SIGMET's RVP7/IFD) that can simultaneously process the H and V signals for the Joint POLarimetry Experiment (JPOLE) experiment planned for the Spring of 2003. The unique feature of the RVP7/IFD is that it accepts two offset IF signals, one for the H the other for the V component. An alternative approach is to use the same IF frequency but in separate channels starting at the first mixer; this approach will also be investigated at a later time. The RVP7/IFD incorporates sampling (at a high rate) the combined IF signals, digital down conversion, and filtering. Nowadays the device that does these operations is referred to as digital receiver, although in this case the digitization starts at the IF carrier frequency; the microwave receiving circuits remain analog. Digital IF receivers will replace the WSR-88D analog receivers which are rapidly becoming obsolete. The modifications to the WSR-88D required to implement the augmentation described herein are constrained so that no change is made to the signal processing currently in the WSR-88D. That is, the present processors must be allowed to continue to process the H polarized weather signals, and there cannot be any changes to the basic timing circuits that establish the PRTs and sample spacings, and control the display of data. Retaining the present functionality of the radar is necessary in order to test other hardware and software modifications that could have a more immediate impact on the operational WSR-88Ds.

2.2 THE PROPOSED SCHEME

In the proposed scheme, there are two STAble Local Oscillators (STALOs) centered on two different frequencies that, in the down conversion at the first mixers, generate two signals s_H, and s_V at intermediate frequencies, IF_H and IF_V. These two signals are linearly summed and simultaneously sampled at rate f_s of about 35 MHz, the nominal sampling frequency of SIGMET's Intermediate Frequency Digitizer (i.e., the IFD). Because the proposed IF frequencies are well above the SIGMET sampling frequency (the present WSR-88D IF frequency is to be maintained at 57.5490 MHz), the two IF signals will be aliased into the unambiguous frequency interval, $0 \pm f_s/2$ where $f_s/2 = f_N$ is the Nyquist frequency. The aliased spectra need to be far removed from the folding frequencies (i.e, $\pm f_N$) and far from each other to avoid distortion of the aliased signal spectra by digital filters designed to separate the two signals. A separation of at least 4 MHz has been recommended by SIGMET engineers. An optimal arrangement of the sampling frequency and the two intermediate frequencies is achieved if the aliased IF signal spectra are uniformly spaced in the interval $\pm f_N$ (Fig. 2.1; in this figure we do not distinguish $\pm$ frequencies).

Considering that,

(1) there are constraints to use IF_H = 57.5490 MHz that presently exists in the WSR-88D,

(2) the tunable voltage controlled oscillator (VCXO), which determines the sample gate spacing in the RVP7, has a tunable frequency range (with replacement of crystals) between 33.5 to 39.5 MHz, and

(3) the aliased spectra are to be uniformly spaced within the Nyquist bounds,

it is proposed to have all frequencies be harmonics of a fundamental frequency f_o, and that f_o be the WSR-88D's 57.5490 MHz crystal oscillator frequency (i.e., its IF_H) divided by 10 (i.e., f_o = 5.7549 MHz). Furthermore, both IF_H and IF_V as well as the STALOs (i.e., $STALO_H$ and $STALO_V$) need to be phased locked to each other; phase locking is assured if frequencies are harmonics of f_o.

If the sampling frequency f_s is set to be the sixth harmonic of f_o as in Fig. 2.1, the aliased spectrum $S_V^{(a)}$ will be at the frequency of -5.7549 MHz. This is exactly one tenth of the WSR-88Ds Coherent Oscillator (i.e., $COHO_H$) frequency. Because the sampled true spectra at the sampled IF frequencies are aliased about the ± Nyquist frequencies, the S_V spectrum is centered at a frequency 1.1 times IF_H, and 11 times the reference frequency f_o = 5.7549 MHz. That is, the spectra S_H, S_V are respectively centered on the tenth and eleventh harmonics of the fundamental frequency f_o equal to the center frequency of $S_V^{(a)}$. In this scheme the two aliased IF spectra have the spacing of 5.7549 MHz from each other and from the frequencies, 0 and f_N, the Nyquist frequency. This separation should minimize cross- talk and signal distortion, and allow digital bandpass filters to optimally separate the two signal spectra. There are other advantages to the proposed scheme, discussed in Section 2.4, related to the calculation of polarimetric variables and possible frequency drift of the oscillators. The baseband (i.e., the carrier frequency is shifted to zero) Inphase (I) and Quadrature phase (Q) components of the H and V weather signals are generated as described in Section 2.4.

$STALO_V$ and the transmit pulses at IF_H and IF_V, as well as the combined IF_H and IF_V signals, are synthesized in an interface assembly (i.e., the "Dual-pol Frequency Generator"; Fig. 2.2) custom manufactured by SpectraDynamics Inc, Boulder CO. This assembly interfaces the WSR-88D circuits to SIGMET's RVP7/IFD processor so that dual polarimetric (i.e., H, V) data can be collected simultaneously without interfering with the normal operation of the WSR-88D circuits. In the photo of the assembly's front panel (Fig. 2.3a), the input and output connectors are numbered as in Fig. 2.2. Fig. 2.3(b) shows the various sealed boxes that are packaged inside the assembly; each labeled box contains the circuits enclosed by the dashed lines in Fig. 2.2. For example, box B-4 contains the frequency multiplier. *Although Fig. 2.2 gives a block diagram of a method to generate these signals, the actual circuit layout and components used by the vendor might differ from those shown in Fig. 2.2.*

13

The specifications, supplied to the vendor, for the assembly that interfaces the R&D WSR-88D components to the SIGMET RVP7/IFD, are given in Appendix 2.

Fig. 2.2(a) includes circuits that provide down-converted transmitted pulses (i.e, the dual IF burst in Fig. 2.2) to the SIGMET processor. The dual IF burst is necessary because the transmitted phase will be shifted from pulse to pulse if a phase coding scheme is implemented to mitigate range velocity ambiguities (Sachidananda, 2001). The RVP7/IFD allows sampling of the phase of the transmitted pulse in order to reference the phase of the weather signal samples relative to the transmitted one. The down-converted transmitted pulse is derived by mixing the WSR-88D's transmit test pulse, which normally comes from terminal 4A22J7,[1] with $STALO_H$, as shown in Fig. 2.2. Because this RF test pulse normally goes to terminal 4A27J3 on the Ten Position RF Test Switch, a power splitter and amplifier are included in the specifications of the assembly so that their output can pass signals to terminal 4A27J3 without interfering with the normal operation of the R&D WSR-88D.

Fig. 2.2(b) diagrams how IF_V is combined with IF_H to generate a summed dual IF signal that is sent to the SIGMET processor. The IF_V signal is generated by mixing the received vertically polarized signal coming from the V channel of the microwave receiver with $STALO_V$ synthesized from $COHO_H$ and $STALO_H$ as sketched in Fig. 2.2(a). The RF and IF amplifiers, and a mixer pre-amplifier for the V channel, are standard WSR-88D components, and are the same as those used for the H channel. The IF_H signal from the WSR-88D passes to a power splitter and buffer amplifier to be returned to the WSR-88D (i.e., the path from "4" to "9") so that the normal operation of the WSR-88D is not compromised.

The measured bandwidth of the WSR-88D mixer and IF amplifiers (i.e., component 4A5) is sufficiently large (Fig. 2.4) that these can be used for both the IF_H and the IF_V signals. In making the bandwidth measurements, the rf input was maintained at a -19 dBm level and the STALO level was set at the specified level of +3 dBm. The output was measured at J3 and thus the frequency response includes the IF amplifiers that are part of 4A5. (Note that in the proposed setup, the IF signals will be taken from jack J4 which bypasses the amplifiers; thus the bandwidth could be larger).

Note that the interface assembly does not contain any provision to generate the COHO signal for the V channel IF (i.e., $COHO_V$) that could be used to down convert analog IF_V signals to baseband as is presently done in the WSR-88D for the IF_H signals. An analog $COHO_V$ is not required because the digital receiver of SIGMET's RVP7/IFD does not require continuous wave (CW) analog COHO signals to generate the baseband In-phase (I_H, I_V) and Quadrature phase

---

[1]Terminal designations are those used in the WSR-88D drawings of the transmitter/receiver/test signal paths provided by the NWS Training Center, 4/16/99. For example, the first four digits identifies a particular component, 4A22 is the Four Position Diode Switch, and the last two digits, J7, is jack number 7 on this component

(Q_V, Q_H) components of a weather signal; these baseband I and Q components are digitally derived as explained in Section 2.4.

The transmitted frequency f_t has a nominal value of 2705 MHz which is obtained from a crystal oscillating (independently of the COHO) at a frequency f_x of about 115 MHz (Fig. 2.5). The band of f_x frequencies in this figure designates the range of frequencies that are used in the network of WSR-88Ds to synthesize the transmitted frequencies in the band from 2700 to 3000 MHz. This figure shows the steps used in the WSR-88Ds to generate $STALO_H$, the $COHO_H$ = IF_H, and the transmitted frequencies. In the proposed arrangement (Fig. 2.2), $STALO_V$ frequency is set to be $1.1 \times COHO_H$ = 63.3040 MHz above the transmit frequency (Fig. 2.2), whereas the $STALO_H$ frequency is, as in the WSR-88D, 57.5490 MHz = $COHO_H$ below the transmit frequency (Fig. 2.5). Therefore, the I, Q signal components in the H and V channels are conjugate and a change in the sign of either I or Q (for one of the channels) is made by the SIGMET processor before computation of the polarimetric variables.

2.3 CONSIDERATIONS FOR PHASE LOCKING IF_H AND IF_V

Because $IF_V = 1.1\ IF_H$ is not an integer multiple of IF_H, there is the possibility that samples of the two IF signals will not be phase locked (i.e., synchronized). To demonstrate, consider the simultaneous transmission of an H, V polarized cw microwave signal (for the R&D WSR-88D, this is at about 2705 MHz) and the simultaneous reception of the H and V echoes from stationary scatterers. There needs to be two mixers and two STALOs. Assume that $STALO_H$, oscillates at a frequency IF_H below the transmitted microwave frequency, and that $STALO_V$ oscillates at IF_V above the transmitted frequency. Since both STALOs frequencies are derived from the same crystal oscillator (i.e., IF_H), the two STALO frequencies will be separated precisely by $2.1\ IF_H$ or $21f_o$.

Let's digress for the moment and consider the phase shifts in the received microwave signal and those in the corresponding down-converted signal at IF_H. Although the IF_H signal is sampled, the phase *shifts* of this signal will be exactly the same as if the microwave signal was sampled. Because there are added phase shifts due to the mixer and associated receiver circuits, the phase of the sampled IF signal might differ from that of the sampled microwave signal, but the phase *shifts* of the sampled microwave signal and of the sampled IF_H signal will be identical (phase shifts that are required for Doppler measurements). For example, if the scatterer moved precisely a quarter of a wavelength of the microwave signal, the phase of a sampled microwave signal would shift by 180°. Likewise, the phase of the sampled IF_H signal will also shift by 180°, as would the phase of the baseband I_H, Q_H components. Even though the IF frequency of the V signals differs from that for the H signal, the phase shifts for the sampled IF_V are the same.

We now need to distinguish samples of the IF signal taken at a rate f_s and samples of the IF signal spaced a PRT apart. If the sampling gates are referenced to the start of the transmit pulse, these latter samples are associated with signals from a fixed range, and they lie along what

15

is called the sample-time axis (Doviak and Zrnic, 1993, Section 3.4). That is, along the sample-time axis there is a sequence of samples spaced a PRT apart, and these are samples of echoes from scatterers at a range specified by the time delay between the transmitted pulse and the sampling gate. On the other hand, the samples spaced $(f_s)^{-1}$ apart are samples of signals along the range-time axes (Doviak and Zrnic, op. cit.); these determine the range to scatterers. The samples along range-time and those along sample-time are not necessarily synchronized (i.e., the PRT is not necessarily an integer times $(f_s)^{-1}$).

If f_s is not synchronized with the PRT and the scatterers are not moving, the phase of the IF signal samples spaced along the sample-time axis will change although it shouldn't. To obtain the true Doppler shift, zero in this case, it will be necessary to also sample, at fixed delays relative to the start of the PRT cycle, the phase of the transmitted pulse. Thus the transmitted pulse is also mixed to the IF (Fig. 2.2a) so that it can be sampled at f_s. For the case of stationary scatterers, the sampled transmitted pulses would have the same progression of phase shifts (there is a progression of phase shifts if the PRT and COHO signals are not harmonically related), over the sample-time domain, as those for signals from stationary scatterers. The sampled transmitted phases need to be subtracted from the phases of the sampled weather signal to obtain the phase shift due to motion of the scatterers (zero in this case).

Sampling the transmitted phase is crucial for the digital receiver where signals at IF are sampled. But, if the analog signals at IF are down-converted to baseband before sampling the weather signal, as in the WSR-88D, there is no need to sample the transmitted phase. That is, the phases of the baseband I, Q phasors of echoes from stationary scatterers, and as well the phases of the transmitted pulses, do not change from, one PRT to the next if the sampling gates are at a fixed delay relative to the transmitted pulse. Thus, it is not necessary to measure the transmitted phase if analog signals are sampled at baseband. Furthermore, baseband phase is relatively constant over a pulse width (i.e., it will not change more than ± 180°), and small changes in the sampling gate delays (i.e., jitter) will not cause significant phase change; not so if the IF signals are sampled.

If IF signals are sampled, and the PRT is an integer times $(IF_H)^{-1}$ there also would be no need to sample the transmitted phase. In the WSR-88D this could be done because the PRTs are synthesized from a Master Clock having a base period precisely six times the period of the COHO (i.e., $6x(IF_H)^{-1}$). Thus PRT $= n(IF_H)^{-1} = 6k(IF_H)^{-1}$ where n and k are integers. In this case the phase shifts of the IF_H samples would also be phase coherent as they presently are for the baseband I_H, Q_H components in the WSR-88D. Although the phase shifts of I_H, Q_H would be synchronized, or phase locked with the transmitted phase, it can be shown that the phase shifts of I_V, Q_V are not necessarily phased locked. In other words, if a scatterer appears stationary to H polarized waves, it can have an apparent velocity for V polarized waves.

Thus there are two approaches to phase locking both the H and V signals. The first approach is to measure precisely the IF frequencies and then select the coefficients of the

digitally synthesized COHOs so that $COHO_H$ and $COHO_V$ are respectively equal to IF_H and IF_V (at the time of this writing this is approach has been implemented).

Alternatively, if the range-time sampling intervals (i.e., the period f_s^{-1}) of the RVP7/IFD are synchronized with the fundamental frequency f_o, the aliased signal samples $s_V^{(a)}$ and $s_H^{(a)}$, corresponding to the two aliased spectra $S_V^{(a)}$ and $S_H^{(a)}$ in Fig. 2.1, would be phase locked. That is, the phase shifts from sample-time to sample-time (i.e., from one PRT to the next) would be the same for both the H and V signals. The required synchronization is obtained directly by setting IF_H and IF_V to be harmonics of f_o, and the sampling frequency f_s needs to be precisely set to 34.5294 MHz, the sixth harmonic of f_o. If f_s is not equal to $6f_o$, it can be shown that the phase shifts of the V signals will be different from the phase shifts of the H signals.

The advantage of the second approach is that, if the frequencies of the COHOs and STALOs (derived from two different crystal oscillators) change in time due to temperature and/or aging, the two digital COHOs remain phase locked. This is not so for the first approach, where the COHO frequencies would have to be reset as the COHO frequency changes. For high quality crystals in temperature controlled ovens, as in the WSR-88D) the drifts are not expected to be significant (i.e., < 1 Hz per day). On the other hand, if the sampling frequency f_s is not a harmonic of both $IF_H^{(a)}$ and $IF_V^{(a)}$ (the aliased IF frequencies), there are phase jumps from range bin to range bin. Although these phase jumps do not affect measurements confined to each range bin (such as the Doppler moments and many of the polarimetric variables), the calculation of specific differential phase requires continuity of phase. If f_s is not a harmonic of both $IF_H^{(a)}$ and $IF_V^{(a)}$ (as it is at the time of this writing), then the phase jumps need to be corrected (these corrections can be made in the SIGMET processor). But if f_s is a harmonic of both $IF_H^{(a)}$ and $IF_V^{(a)}$, phase shifts from range bin to range bin are continuous, and thus the specific differential phase shift would be a continuous function of range. To have this continuity requires that the range bin size (i.e., the number of samples that are taken to compute the baseband signals I and Q, be a multiple of three.

The RVP7 internal sampling frequency f_s can be set to any value[2] in the range of 33.5 to 39.5 MHz by supplying it a reference signal frequency that is related to f_s, by the following equation (SIGMET's RVP7 User's Manual, p.2-6)

$$f_s = 2\frac{P}{Q}f_{ref}$$

where P and Q are integers in the range 1 to 128, and f_{ref} is an external reference frequency to which the internal clocks of the RVP7 can be synchronized. SIGMET engineers recommend using $COHO_H = 10f_o$ as the reference frequency because it likely has the least phase noise. In this

---

[2]This requires replacement of a voltage controlled crystal oscillator (VCXO) installed in the SIGMET processor. The VCXOs have very narrow tuning range and no one VCXO can span the entire frequency band from 33.5 to 39.5 MHz.

case P and Q calculate to be 9 and 30 respectively, and the H and V signals will be phase coherent with each other.

If the sampling frequency f_s is set precisely to the sixth harmonic of f_o, there would not be a need for the dual burst IF_H and IF_V outputs shown in Fig. 2.2(a). Although the dual burst IF output might not be needed, it is included as a part of the interface because there are plans to phase encode the transmitted pulse to explore techniques to mitigate the effects of overlaid echoes in the WSR-88D (Sachidananda, 2001). In that case, the transmitted phase must be sampled, and the dual burst output allows this capability.

Although the IF_V, IF_H, and f_s are synchronized, the WSR-88D's Master clock, which sets the PRTs, is not synchronized because its frequency, f_{clk}, is not an integer times f_o (i.e., f_{clk} = 1.6666 f_o). Since all the timing circuits in the WSR-88D are derived from the master Clock with a base period of $6(IF_H)^{-1}$, any changes in the Master clock frequency could have serious consequences in all of the programs within the WSR-88D signal processors which assume a predetermined set of PRTs derived from the WSR-88D's Master clock. Thus it is not practical to change the WSR-88D's master clock frequency (i.e., the SIGMET processor needs to be a stand-alone system, without requiring changes to the R&D WSR-88D). But, to assign ranges to the digitally synthesized I, Q phasors, the beginning of the summing operation (used to filter the signal with samples spaced $\Delta t = f_s^{-1}$ apart; section 2.4) needs to be reset every PRT to be in synchronization with the transmitted pulse. Thus, the SIGMET processor requires PRT clock pulses so that the digital I, Q samples can be assigned ranges.

2.4 THE GENERATION OF INPHASE AND QUADRATURE PHASE COMPONENTS, AND MATCH FILTERING

Fig. 2.6 shows in block diagram how digital mixers synthesize baseband digital samples of I_H, Q_H, and I_V, Q_V. The analog to digital converter (A/D) samples the summed IF_H and IF_V analog signals, and generates 12 bit digital words at the rate $6f_o$ = 34.5294 MHz. Although the analog H and V signals are at the IF frequencies $COHO_H$ = 57.5490 and $COHO_V$ = 63.3039 MHz respectively, these signals are under-sampled which is equivalent to sampling aliased IF signal spectra centered on f_o = -5.7549 and on $2f_o$ = -11.5098 MHz (i.e., the aliased signals $s_V^{(a)}$ and $s_H^{(a)}$). Thus, the samples of $s_V^{(a)}$ will occur at intervals of about 60° (exactly 60° if the scatterers are stationary) because the sampling frequency is 6 times the center frequency of $S_V^{(f)}$, and the samples of $s_H^{(a)}$ will be spaced about 120° because the sampling frequency is 3 times the center frequency of $S_H^{(f)}$. That is, there will be six samples every period of $s_V^{(a)}$, and three samples for every period of $s_H^{(a)}$. Nevertheless, both H and V signals are sampled simultaneously and each sample is of the summed $s_H + s_V$ signals. The digital band pass filters are designed to pass only the H or V components of the summed signal samples in their respective channels.

The next step is to multiply the band-passed V digital samples by $a_n \sin\theta_{nV}$ and $a_n \cos\theta_{nV}$, where $\theta_{nV} = 360(n - 1)IF_V \Delta t$; $IF_V = 11f_o$, $\Delta t = (6f_o)^{-1}$, and $n = 1, 2, 3, \ldots\ldots$ Thus $\theta_{nV} = (n-1)660° =$

18

$(n - 1)300°$. The coefficient values a_n can be selected to obtain a prescribed range weighting function; typically the amplitudes have a variation equal to the variation of the transmitted pulse. For example, if the transmitted pulse is rectangular in shape, and all coefficients were equal with the length of the sample sequence equal to the pulse width, the result would be a matched filter, and the range weighting function would be triangular in shape with a base equal to twice the pulse width. Likewise the band-passed H digital samples are multiplied by $a_n\sin\theta_{nH}$ and $a_n\cos\theta_{nH}$, where $\theta_{nH} = 360(n - 1)IF_H\Delta t$. In this case $\theta_{nH} = (n - 1)240°$. The digitally synthesized I_V and Q_V are obtained from the sums:

$$Q_V = \sum_1^N a_n\sin(\theta_{nV})A_V\sin[(2\pi IF_V+\omega_d)(n-1)\Delta t + \phi_V]$$

$$I_V = -\sum_1^N a_n\cos(\theta_{nV})A_V\sin[(2\pi IF_V+\omega_d)(n-1)\Delta t + \phi_V]$$

where $\Delta t = (f_s)^{-1}$, $A_V\sin[(IF_V+\omega_d)(n-1)\Delta t + \phi_V]$ is the digital number representing the analog signal in the IF_V channel, ω_d is the Doppler shift, A_V is the time varying amplitude, and ϕ_V is an unknown phase shift related to the time delay from the transmitted pulse to the sampling gate; this determines the range to the scatterers that contribute to the signal sample. The negative sign in front of the sum for I_V is required because the aliased frequencies of $s_V^{(a)}$ and $s_H^{(a)}$ are negative.

There is a similar equation for I_H and Q_H, except that the increments of phase advance by θ_{nH}, the IF frequency would be IF_H, and the signal phase would be ϕ_H, not necessarily equal to ϕ_V if there is different phase shift along the path, and upon scattering.

As stated earlier, the number N of product samples to be summed and the values of the weighting parameter a_n depend on the matched filter characteristics. For the R&D WSR-88D the transmitted pulse is approximately rectangular and has a width of about 1.6 µs If a_n were a constant independent of n (e.g., $a_n = 1$), N would have to be about 56 samples (i.e., $56 \times \Delta t = 1.6$ µs) to have a filter that is matched to the transmitted pulse.

3. LIST OF REFERENCES

Doviak, R. J., and D. S. Zrnic, 1993: *Doppler Radar and Weather Observations*. Academic Press, San Diego, CA, 562 pp.

Doviak, R. J., D. S. Zrnic, J. Carter, A. Ryzhkov, S. Torres, and A. Zahrai, 1998: Polarimetric Upgrades to Improve Rainfall Measurements. Report of the National Severe Storms Laboratory, Norman, OK 73069, 110 pp.

Kefalas, G. P., and J. C. Wiltse, 1970: Transmission Lines, Components, and Devices, in *Radar Handbook*, M. I. Skolnik, Editor in Chief, McGraw-Hill, New York, pp.8-1 to.8-8-38.

Pratt, F., and D. Ferraro, 1995: Improved WSR-88D Sun-Source Calibration Software and Procedures: Analysis, Recommendations, and Test Plan. Final Eng. Rept. FY95 to the NWS Operational Support Facility, Norman, OK, 66 pp.

Sachidananda, M., 2001: Signal Design and Processing Techniques for WSR-88D Ambiguity Resolution. Part-5: Further Investigation. National Severe Storms Laboratory Report, Norman, OK., 75 pp.

Skolnik, M. I., 2001: *Introduction to radar systems*, 2nd edition, McGraw-Hill, Boston,772 pp.

Zrnic, D. S., A. Ryzhkov, J. Straka, Y. Liu, and J. Vivekanandan, 2001: Testing a Procedure for Automatic Classification of Hydrometeor Types. Jo. Atmos. & Oceanic Tech., **18**, 892-913.

APPENDIX 1: SPECIFICATIONS FOR THE DUAL CHANNEL ROTARY JOINT AND WAVEGUIDE ASSEMBLIES

The modification of the WSR-88D antenna to allow dual polarization measurements using simultaneous transmissions of H and V polarized signals created a need for a dual channel azimuthal rotary joint and an additional single channel elevation rotary joint.

A dual channel azimuth rotary joint (Fig. A1.1) was selected so that the H and V channel microwave components (e.g., the switches, circulators, terminations, and power splitters in Fig. 1.2) could be located at the base of the pedestal and thus be readily accessible for testing, maintenance, and modification. In a permanent configuration, a single channel azimuthal rotary joint could be used if all the microwave components were located atop or in the elevation drive housing. In that case, the WSR-88D's azimuthal rotary joint would need three coaxial channels for rf signals; two for the H and V microwave signals from the circulators (or the LNAs if the front end receiver components were also located atop the elevation housing to lower the noise levels), and one for the calibration signal. In any future design, this configuration should be examined carefully because radar performance might be improve if the number of waveguide bends and flexible guides is reduced, and if the LNAs are located closer to the antenna port.

The electrical specifications for the dual channel azimuth rotary joint are:

1) Frequency range: 2.7 to 3.0 GHz

2) Maximum power (with pressurization of 5 psig of dry air)

    a) inner channel for vertically polarized signals: 550 kW
    b) outer channel for horizontally polarized signals: 1.1 MW
        (2.2 kW average power with pulse widths between 0.7 and 5μs)[3]

3) Isolation between vertical and horizontal channels: >50 dB
    (If higher isolation is required conducting gaskets could be used)

4) Loss Factors:
    a) outer H-channel: < 0.1 dB
    b) inner V-channel: < 0.2 dB

5) VSWR in each channel: < 1.2
    WOW (change of VSWR for 360° change in azimuth):   < 0.08

6) The rotary joint should be capable of holding a pressure of 10 psig

---

[3] The specifications for the outer or H channel satisfy the requirements for the WSR-88D.

To fit two waveguides inside the torque tube (a 85.5 inch long cylinder that delivers azimuth torque to rotate the WSR-88D's reflector) a specially fabricated dual channel waveguide assembly (Fig. A1.2) was required. One end of the waveguide assembly attaches to the output of the dual channel azimuth rotary joint and the other end attaches to a specially fabricated dual channel 90° waveguide bend (Fig. A1.3a). This waveguide bend was required to exit the elevation drive housing and to mate with standard waveguides leading to the elevation rotary joints. The dual channel 90° bend is located in the elevation drive housing on top of the antenna pedestal. A photograph of the dual-channel 90° bend inside the elevation housing is shown in Fig. A1.3(b). The large flange is the output side (in the transmit mode) of the dual-channel 90° bend.

Fig. A1. 4 is a photograph of the elevation housing showing waveguides connected to the output of the dual-channel 90° bend. The H channel has standard rigid guides going to the rotary joint (not visible in this photograph), but the V channel has a long flexible guide that joins the output of the dual-channel 90° bend to the vertical channel rotary joint. Also seen in this figure is the flexible guide that connects the vertical channel rotary joint to the vertical channel waveguide that leads to the rigid waveguide strut located at the edge of the reflector. Thus the V channel has more flexible guides than the H channel and thus might have larger loss. A permanent configuration would use rigid waveguides to minimize loss.

The two elevation rotary joints are simply a pair of standard WSR-88D rotary joints mounted on opposite sides of the elevation axis and thus they meet all the specifications for the WSR-88D.

APPENDIX 2: SPECIFICATIONS FOR THE INTERFACE BETWEEN THE R&D WSR-88D AND THE SIGMET RVP7/IFD SIGNAL PROCESSOR

The interface between the WSR-88D receiver and the SIGMET processor is an interim solution to allow polarimetric data collection with the Research WSR-88D for supporting NWS experiments (e.g., the Joint POLarization Experiment, JPOLE) until a dual polarization mode is installed in the Open Radar Data Acquisition (ORDA) unit. In this interim configuration, normal operation of the WSR-88D is allowed for testing upgrades to the network of WSR-88Ds, while polarimetric data are collected with the SIGMET RVP7/IFD processor.

Fig. A2.1 shows all the inputs and outputs that are *required* to interface the WSR-88D to the SIGMET processor without interfering with the normal operation of the WSR-88D, as well as other outputs that were added for possible future use (for example, number 13, the spare COHO H signal). Although this is shown as a single component with multiple inputs and outputs, the vendor supplied interface is composed of ten units, individually packaged to minimize coupling between signal paths. But all packages are placed into a single box (Fig. 2.3) for rack mounting.

Inputs for the interface that are derived from the WSR-88D are:

1. A 57.5491MHz COHO signal ($COHO_H$) at a power level of -3 dBm from terminal 4A10 J3 (terminal designations are those used in the WSR-88D drawings of the transmitter/receiver/test signal paths provided by the NWS Training Center, 4/16/99. For example, the first four digits identifies a particular component, 4A10 is the phase detector, and the last two digits, J3, is jack number 3 on this component).

2. A 2647.4509 MHz STALO signal ($STALO_H$) at a power level of -13dBm from terminal 4A5J6 of the mixer pre-amplifier.

3. A 2705.0 MHz RF TEST PULSE which is the transmitted frequency pulse-modulated at a power level of -7 dBm from terminal 4A22J7 of the Four Position Diode Switch.

4. A 57.5491 MHz IF signal from the WSR-88D H channel mixer/pre-amplifier at terminal 4A5J4.

5. A 63.30401 MHz IF signal from the WSR-88D V channel mixer/pre-amplifier at terminal J4.

6. DC POWER SUPPLIES . +/- 9V, +/- 18 V, +5V.

23

These RF and IF signals, that are taken by interrupting a signal path in the WSR-88D, are required to pass out of the interface through buffer amplifiers and be returned to the WSR-88D to its originally intended destination.

Interfacing the dual polarization WSR-88D to the SIGMET RVP7 signal processor requires the generation and availability of several RF signals (Fig. A.2.1):

7. A STALO$_V$ signal at a frequency of 2768.30401 MHz (in order to generate a second IF, IF$_V$, at a frequency of 63.30401 MHz) at a power level in the range of +14 to +17dBm. It is to be derived from the WSR-88D CW COHO signal (i.e., COHO$_H$) and the WSR-88D CW STALO signal (STALO$_H$) according to the following relation;

$$STALO_V = 2.1 * COHO_H + STALO_H$$
$$STALO_V = ((57.5491 \text{ MHz} * 21/10) + 2647.4509 \text{ MHz}) .$$

STALO$_V$ must be phase locked to COHO$_H$

8. A dual IF BURST SIGNAL which is the linear sum of two burst signals at IF$_H$ and IF$_V$ with a power level of 0 dBm. This signal should be derived from the 2705 MHz RF TEST signal, STALO$_H$, and STALO$_V$ signals, and be phase coherent with the WSR-88D transmitted signal at 2705 MHz.

9. A buffered 57.5491 MHz IF signal to be applied to terminal 4A14J1 of the Guard Band Amplifier (device 4A14). The level of this IF signal can vary over the power range of approximately 0 to -90 dBm.

10. An IF signal composed of the linear sum of the two IF signals IF$_H$ and IF$_V$ that are phase and amplitude balanced. The level of this IF signal can vary over the power range of approximately +3 to –87 dBm.

11. A buffered 57.5491 MHz COHO signal at a nominal power level of 0 dBm that will be used as the sampling clock input to SIGMET's RPV7/IFD.

12. A buffered 57.5491 MHz COHO signal at a nominal power level of -3 dBm that will be applied to terminal 4A28J5 of the Ten Position IF Test Switch.

13. A buffered 57.5491 MHz COHO signal at a nominal power level of -3 dBm that will be a spare COHO$_H$ to be used for development of a digital receiver for the WSR-88D.

14. A buffered 2647.4509 MHz STALO$_H$ signal at a power level in the range of -15 to -13 dBm to terminal 4A27J2 of the Ten Position RF Test Switch.

24

15. A buffered 2705 MHz RF test signal at a power level of -7dBm +/-1.25 dB to terminal 4A27J3 of the Ten Position RF Test Switch.

The above numbers correspond to those seen both in Fig. A2.1 as well as in Figs. 2.2 and 2.3.

OTHER ELECTRICAL SPECIFICATIONS FOR THE INTERFACE

VSWR:
All input/output signal ports shall present a nominal impedance of 50 ohms with a VSWR less than 1.3:1 .

OUTPUT ISOLATION:
Buffered RF outputs shall provide a minimum of 20 dB load isolation. Buffered IF outputs shall provide 25 dB of reverse isolation.

Cross- CHANNEL ISOLATION:
80 dB minimum between the lines containing $STALO_V$, $STALO_H$, buffered $STALO_H$, RF Test, and buffered RF Test signals.

HARMONIC OUTPUT:
All output signals shall have 2nd harmonic levels at -60 dBc maximum. All other harmonic levels must be -70 dBc Maximum.

SPURIOUS OUTPUTS:
All RF signals must have non-harmonically related outputs below -70dBc in the range +/- 80 MHz from the carrier.

All IF signals must have non-harmonically related outputs below -80 dBc over a frequency range of +/- 10 MHz from the IF carrier.

FM Noise on $STALO_V$ and the buffered $STALO_H$ signals (See Fig. A2.2 for specifications).

AM Noise on $STALO_V$ and the buffered $STALO_H$ signals (see Fig.A2.3 for specifications).

RADIO FREQUENCY INTERFERENCE:

The unit shall be shielded such that the leakage radiation measured within one inch of any surface of the unit shall be at least 80 dB down from the maximum output signal. The leakage measurement shall be made using a flange mount "N" type connector with the center conductor extended one quarter wavelength at 2.85GHz and connected to a spectrum analyzer.

INTERNAL OVER VOLTAGE PROTECTION:
The unit shall not be damaged and shall continue to meet requirements of this specification for a supply over voltage condition as follows with a duration not to exceed 50 microseconds.

SUPPLY VOLTAGE	OVER VOLTAGE(max)
+18 VDC	+21 V
- 18 VDC	- 21 V
+ 5 VDC	+ 7 V
- 9 VDC	- 12 V
+ 9 VDC	+ 12 V

CONNECTORS:
Signal connectors shall be flange mounted type SMA female.
The power supply connector shall be a 15 pin subminiature male D connector.

ENVIRONMENTAL CONDITIONS:
Temperature range:
Operating: 0 deg C to +50 deg C
Non-operating: -35 deg C to +60 deg C
Humidity range:
Operating: 15 - 80%
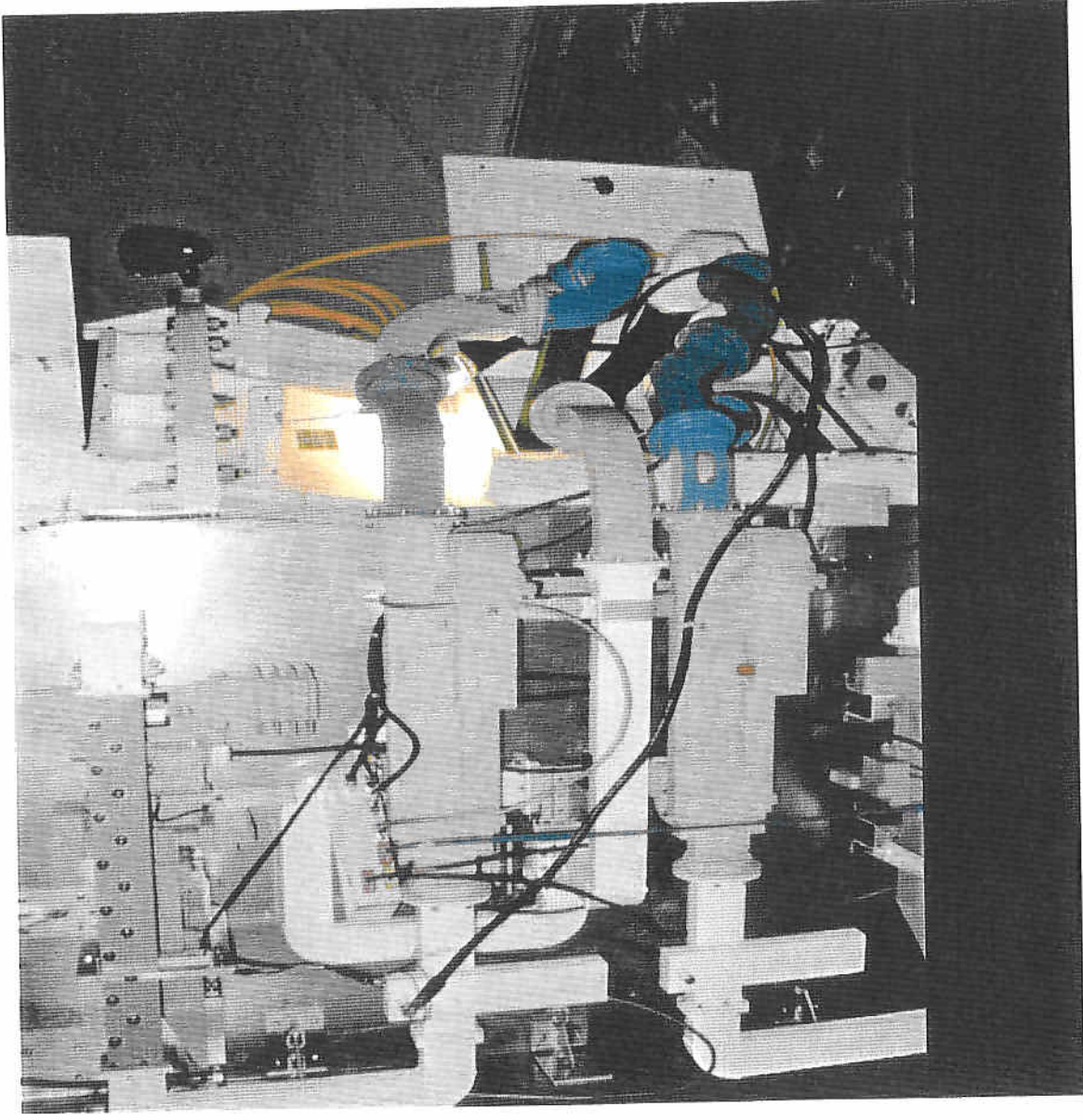Non-operating: 15 - 100%

List of Figure captions

Fig. 1.1(a) Some of the microwave components used in switching between H transmissions, but with simultaneous reception of H,V polarized echoes, and simultaneous transmissions and reception of H,V polarized echoes.
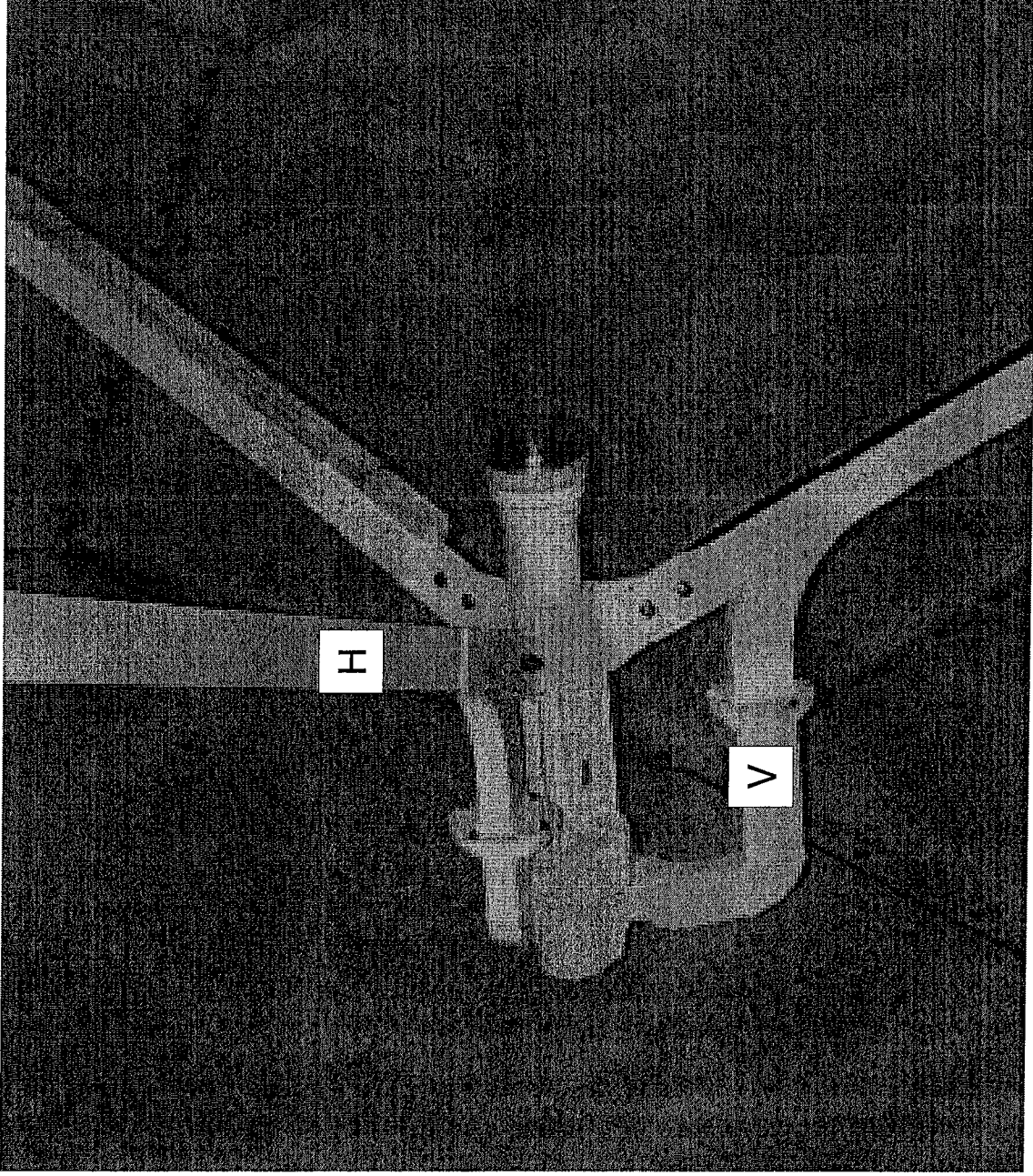
Fig. 1.1(b) The feed that illuminates the antenna reflector with H and V polarized waves. Two of the struts supporting the feed are wave guides that transport the H and V waves. The narrow walls of the guides face the reflector to minimize blockage.

Fig. 1.2 Schematic of the microwave components used to switch between single mode transmissions and simultaneous transmission and reception of H, V waves. Switches are in the position for simultaneous transmission and reception. Encircled numbers indicate ports where insertion loss measurements are made.

Fig. 1.3 Same as Fig.1.2, except the switches are set to transmit only H polarized waves, but to receive both H and V waves.

Fig. 2.1 The proposed arrangement of sampled and aliased IF signal spectra $S_V^{(a)}$, $S_H^{(a)}$ of the vertically and horizontally polarized weather signals, the sampling frequency f_s, the COHO frequencies IF_H and IF_V, the Nyquist frequency f_N, and the WSR-88D system (master) clock frequency f_{clk}.

Fig. 2.2(a) A proposed interface between the WSR-88D and the SIGMET RVP7/IFD processor, and a method to synthesize STALO$_V$ and the down-converted transmitted pulses at IF_H and IF_V (i.e., the dual IF bursts).

Fig. 2.2(b) A block diagram of circuits to combine the IF_H and IF_V weather signals.

Fig. 2.3(a) The front panel of the Dual-Pol Frequency Generator that interfaces the WSR-88D radar to the SIGMET RVP7/IFD processor. The numbers associated with each connector correspond to the circled numbers in Fig. 2.2.

Fig. 2.3(b) An inside view of the Dual-Pol Frequency Generator showing the various boxes containing the circuits drawn in Fig. 2.2. The box labels correspond to the circuits enclosed by the dashed lines in Fig. 2.2

Fig. 2.4 The measured frequency response of the WSR-88D mixer-preamplifier designated 4A5.

Fig. 2.5 A block diagram of the circuits used to synthesize the STALO$_H$, COHO$_H$, and the RF DRIVE (i.e., the transmitted) signals in the WSR-88D.

Fig. 2.6 A block diagram of a digital receiver that samples two summed signals $s_H + s_V$, at the intermediate frequencies 57.549 and 63.3049 MHz respectively, and generates I_H, Q_H, and I_V, Q_V at baseband.

Fig. A1.1(a) A schematic of the dual channel azimuth rotary joint.

Fig. A1.1(b) A photograph of the dual channel azimuth rotary joint. The lower two wave guides are the inputs. The output waveguides at the top connect to the dual channel waveguide assembly (Fig. A1.2) that passes through the torque tube.

Fig. A1.2 A schematic of the dual channel waveguide assembly that passes through the torque tube.

Fig. A1.3 a) A schematic of the dual channel 90° waveguide assembly.

Fig. A1.3 b) The dual-channel 90° waveguide bend inside the elevation drive housing.

Fig. A1.4 Photograph of the elevation drive housing. The output of the dual-channel 90° waveguide assembly is connected to the waveguides which lead to the elevation rotary joints and then to the waveguide struts supporting the antenna feed shown in Fig. 1.1(b).

Fig. A2.1 A block diagram showing the output connectors of the Dual-Pol Frequency Generator connected to the various circuits of the WSR-88D and the SIGMET processor.

Fig. A2.2 The specifications of the allowable FM noise on the $STALO_V$ and the buffered $STALO_H$ signals.

Fig. A2.3 The specifications of the allowable AM noise on the $STALO_V$ and the buffered $STALO_H$ signals.

Fig. 1.1 (a) Some of the microwave components used in switching between H transmissions, but with simultaneous reception of H,V polarized echoes, and simultaneous transmissions and reception of H,V polarized echoes

Fig. 1.1 (b) The feed that illuminates the antenna reflector with H and V polarized waves. Two of the struts supporting the feed are wave guides that transport the H and V waves. The narrow walls of the guides face the reflector to minimize blockage.
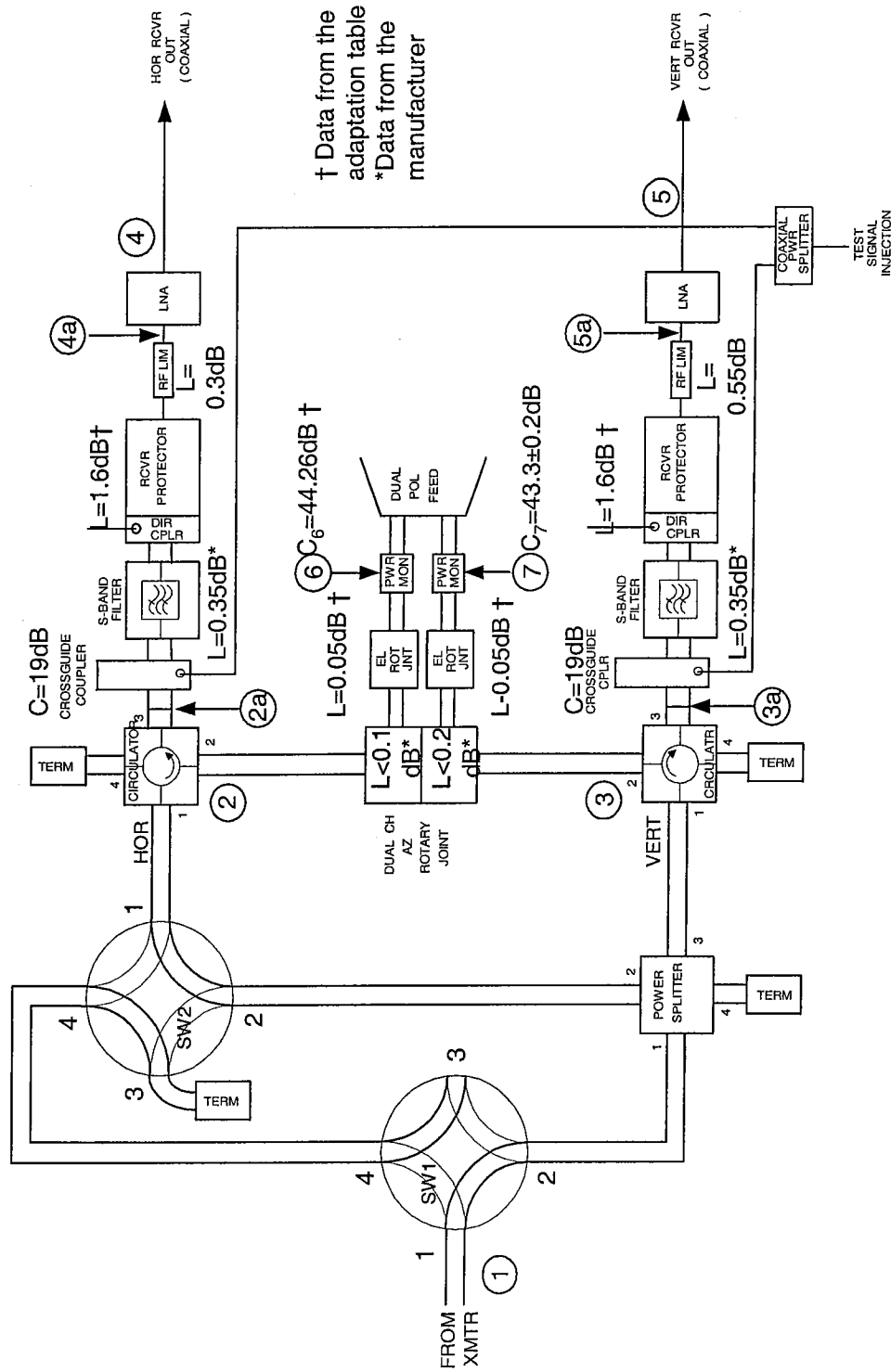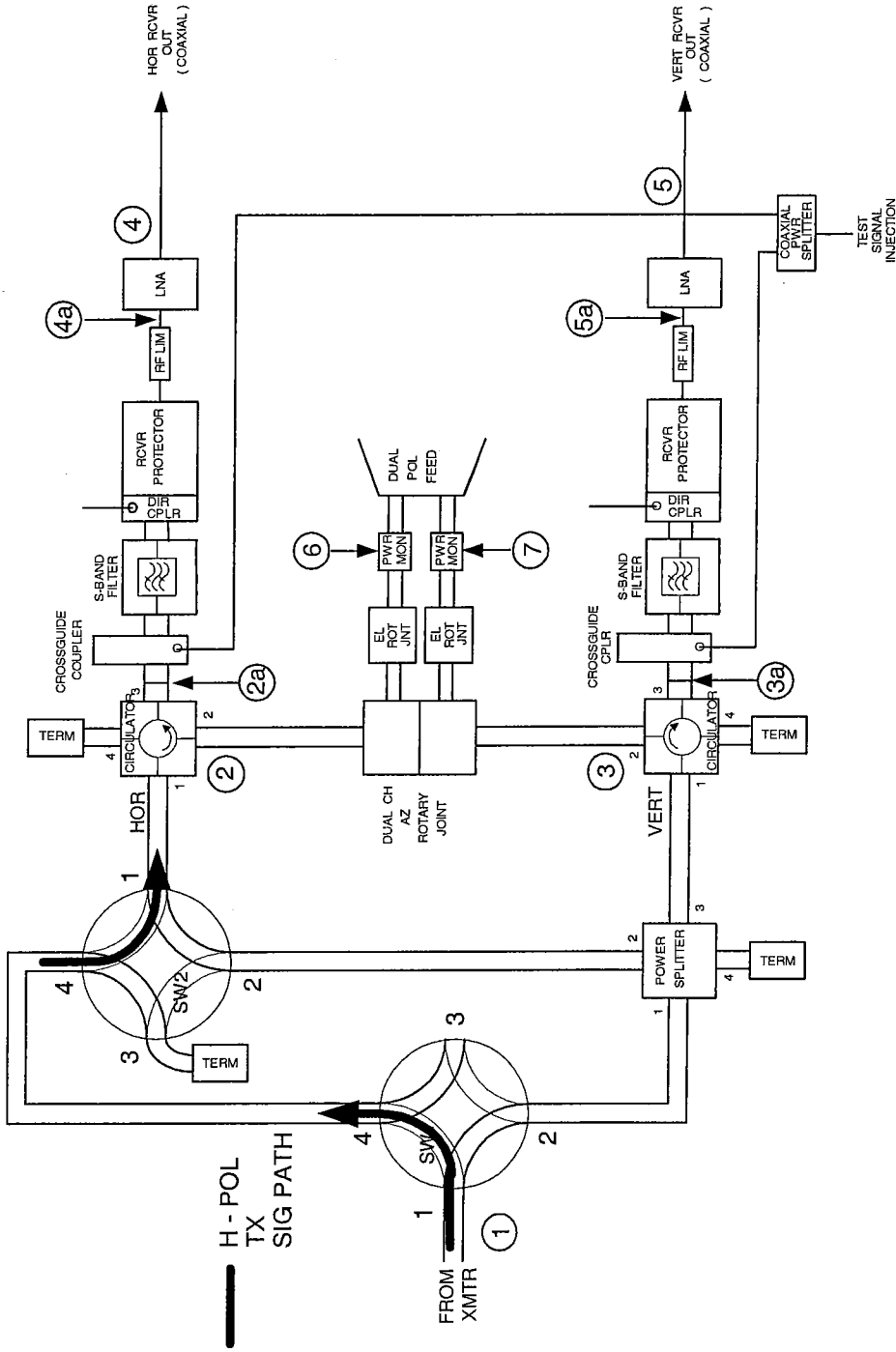
Fig. 1.2 Schematic of the microwave components used to switch between transmissions of H polarized waves with simultaneous reception of both H and V, and simultaneous transmission and reception of H, V waves. Switches are in the position for simultaneous transmission and reception. Encircled numbers indicate ports where insertion loss measurements were made.

Fig. 1.3 Same as Fig. 1.2, except the switches are set to transmit only H polarized waves, but to receive both H and V waves

*WG SW'S S1,S2 SHOWN IN DE-
ENERGIZED POSITION

Fig. 2.1 The proposed arrangement of sampled and aliased IF signal spectra $S_V^{(a)}$, $S_H^{(a)}$ of the vertically and horizontally polarized weather signals, the sampling frequency f_s, the COHO frequencies IF_H and IF_V, the Nyquist frequency f_N, and the WSR-88D system (master) clock frequency f_{clk}.

Fig. 2.2(a) A proposed interface between the WSR-88D and the SIGMET RVP7/IFD processor, and a method to synthesize STALO$_V$ and the down-converted transmitted pulses at IF$_H$ and IF$_V$ (i.e., the dual IF bursts).

IFH INPUT FROM 4A5J4

J5 ④

TO 4A14J1

J4 ⑨

IFV INPUT FROM V CHAN MIXER/PREAMP 4A5J4

J1 ⑤

J2 ㉒

PWR SPLTR

AMP

57.5491 MHz BPF BW = 10MHz

AMP

PWR SPLTR

AMP

63.30401MHz BPF BW = 10MHz

AMP

B-3

J5 ⑩

DUAL-POL IF SIG TO SIGMET PROCESSOR RVP7/IIFD

Fig. 2.2 (b) A block diagram of circuits to combine the IF_H and IF_V weather signals.

Fig. 2.3 (a) The front panel of the Dual-Pol Frequency Generator that interfaces the WSR-88D radar to the SIGMET RVP7/IFD processor. The numbers associated with each connector correspond to the circled numbers in Fig. 2.2.

Fig. 2.3 (b) An inside view of the Dual-Pol Frequency Generator showing the various boxes containing the circuits drawn in Fig. 2.2. The box labels correspond to the circuits enclosed by the dashed lines in Fig. 2.2

4A5 MXR PRE-AMP BW MEAS. JKC 7-25-00.
LO INPUT +3dBm. SIG IN -19dBm

FREQ (mHZ)

POWER OUT(-1* dBm)

Fig. 2.4 The measured frequency response of the WSR-88D mixer-preamplifier (4A5).

STALO $(16fx + 14*IF) =$
2705 MHz - 57.549 MHz

COHO (IF) = 57.549 MHz

RF DRIVE$(16*fx+15*IF)$
ft ~ 2705 MHz

15 IF

X16

X14

PHASE SHFTR

MODULATOR
(generates rf pulses)

PULSE
SHAPE
CNTRLR

XTAL OSC
f x = 114.75 ->133.5 MHz
KOUN ~ 115 MHz

XTAL OSC
IF = 57.549 MHz

PHASE
CNTRLR

Fig. 2.5 A block diagram of the circuits used to synthesize the STALO$_H$, COHO$_H$, and the
RF DRIVE (i.e., the transmitted) signals in the WSR-88D.

Fig. 2.6 A block diagram of a digital receiver that samples two summed analog signals s_H + s_V at the intermediate frequencies IF(H) = 57.549 and IF(V) = 63.3049 MHz respectively, and generates I_H, Q_H, and I_V, Q_V at baseband.
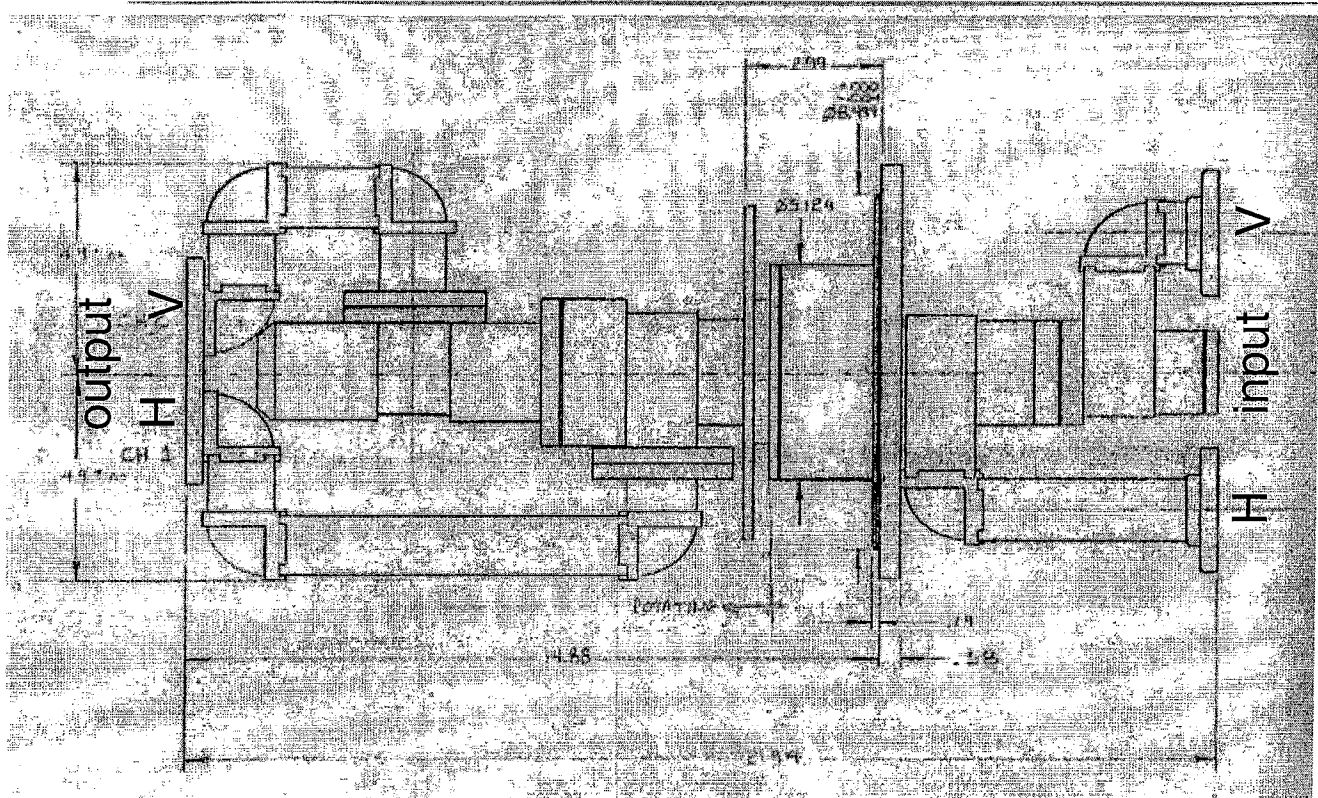
Fig. A1.1 (a) A schematic of the dual channel azimuthal rotary joint

Fig. A1.1 (b) A photograph of the dual channel azimuth rotary joint. The lower two wave guides are the inputs. The output waveguides at the top connect to the dual channel waveguide assembly (Fig. A1.2) that passes through the torque tube.
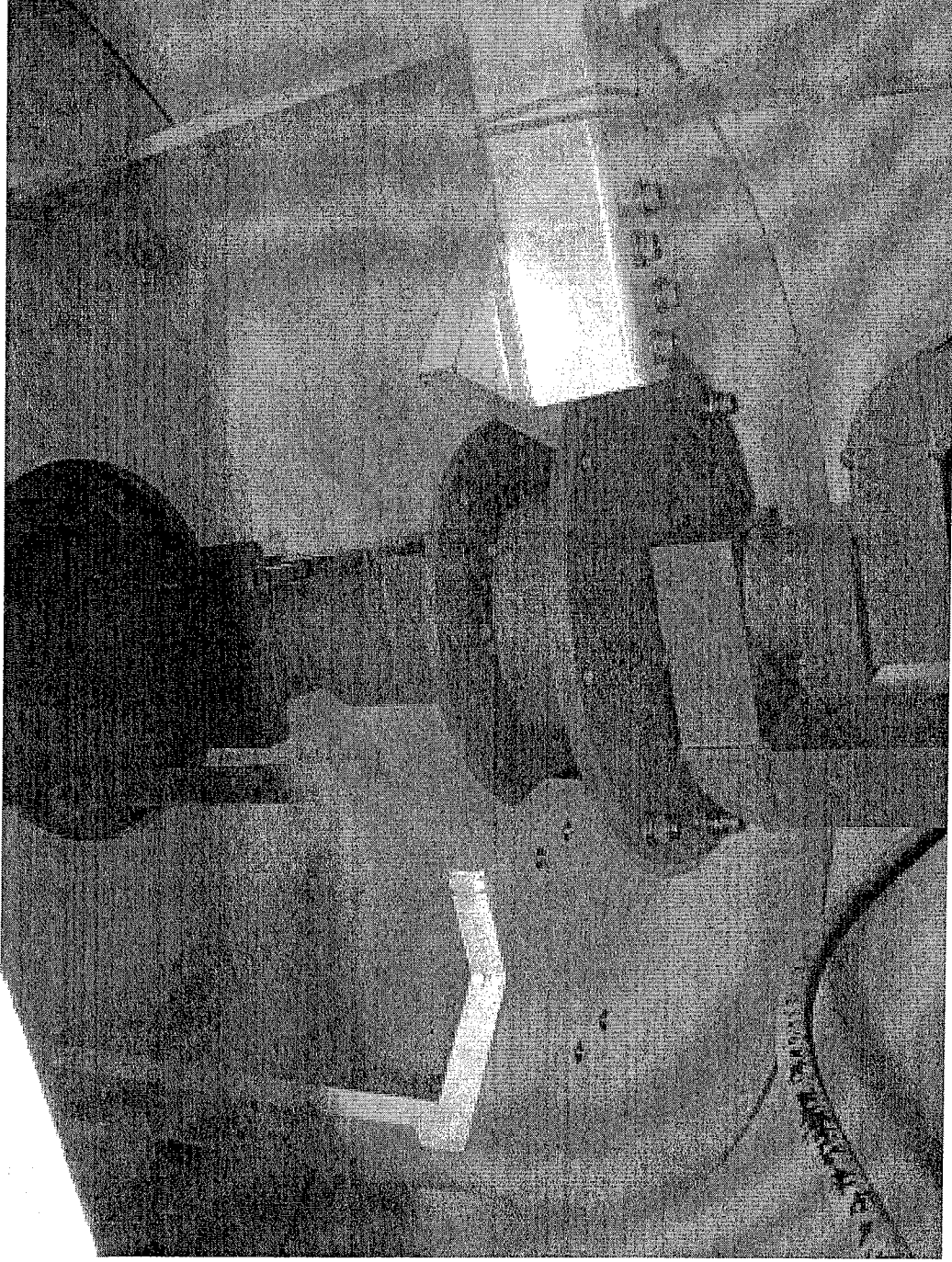
Fig. A1.2 A schematic of the dual channel waveguide assembly that passes through the torque tube.
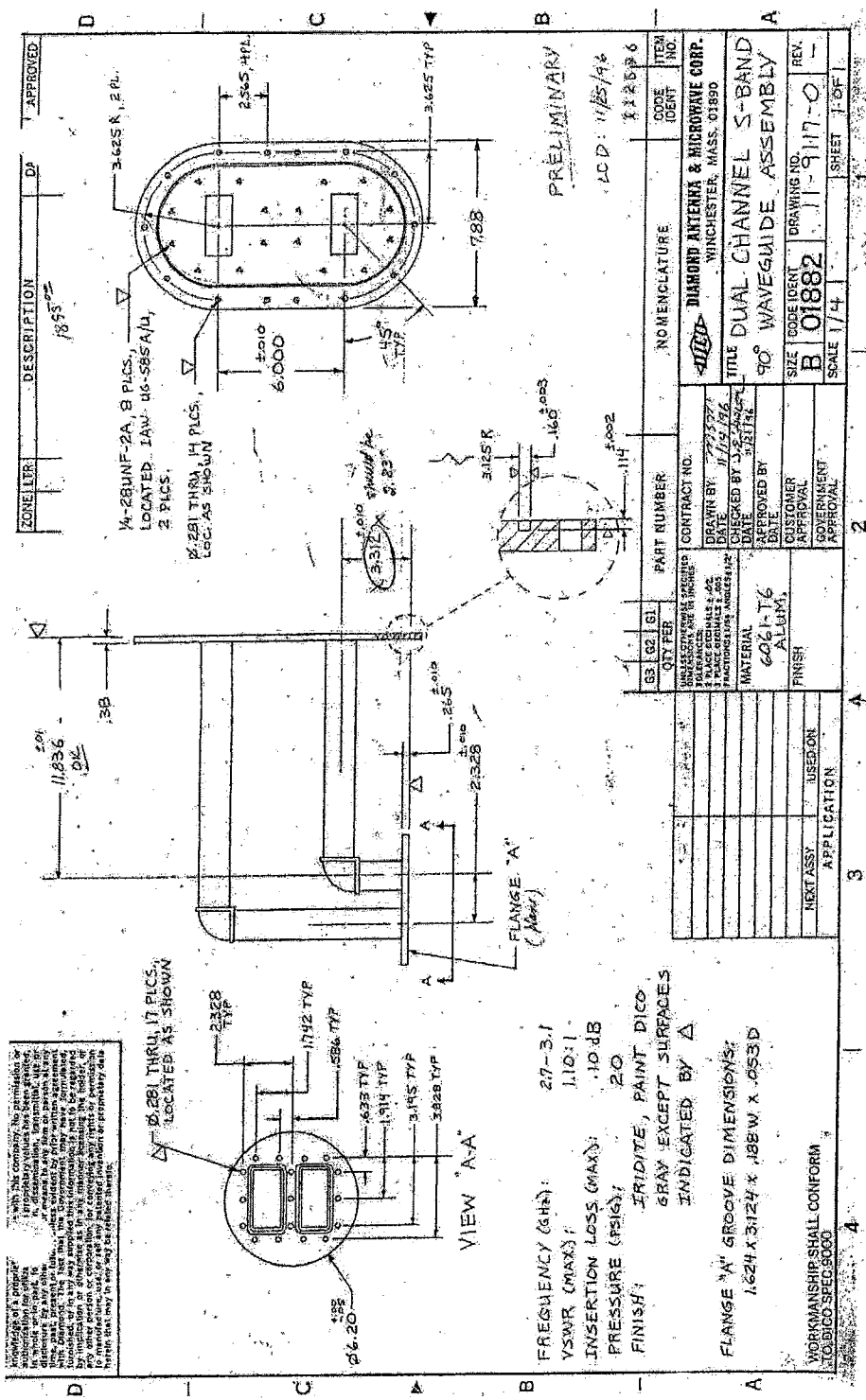
Fig. A1.3 (a) A schematic of the dual channel 90° waveguide assembly.
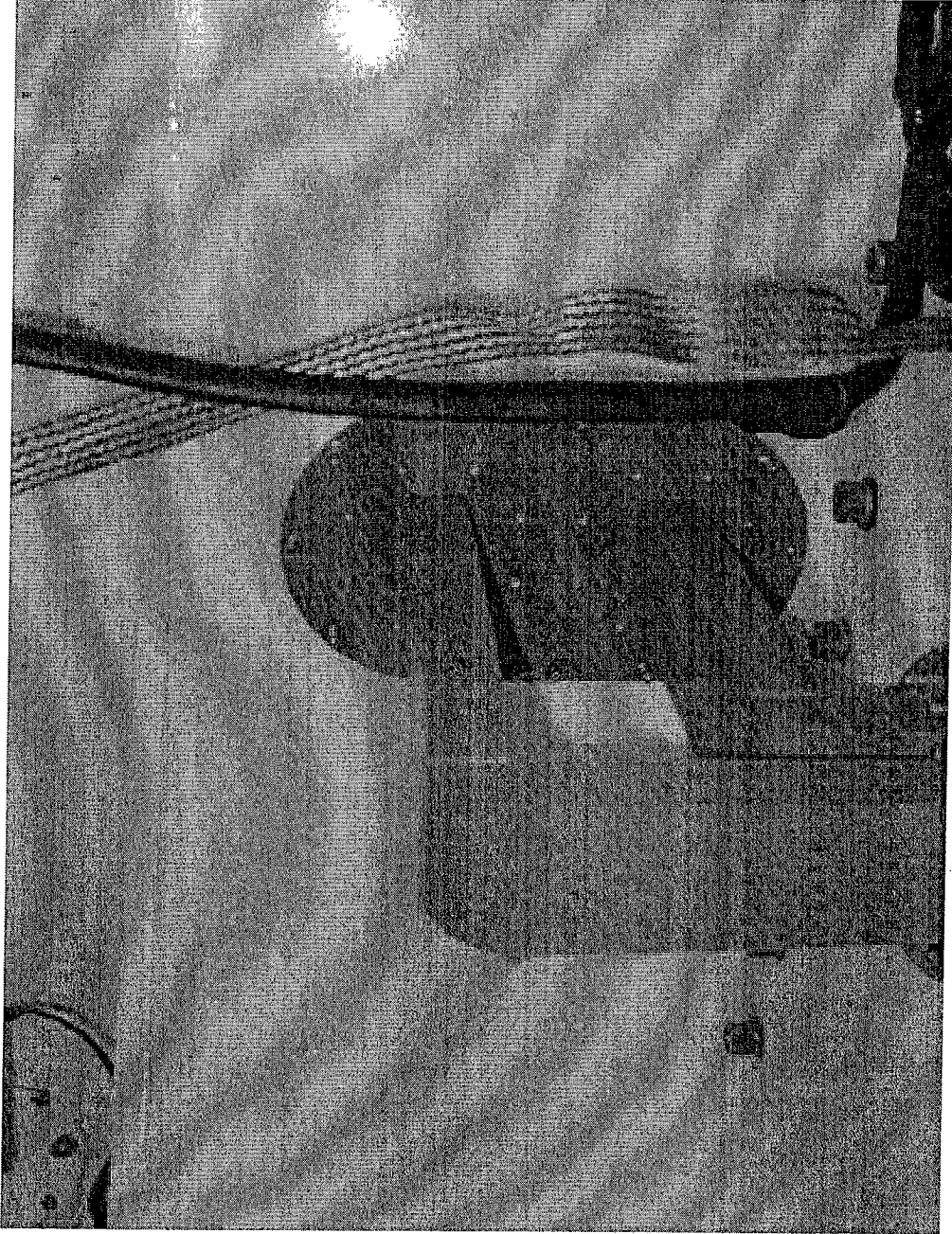
Fig. A1.3 (b) The dual-channel 90° waveguide bend inside the elevation drive housing.
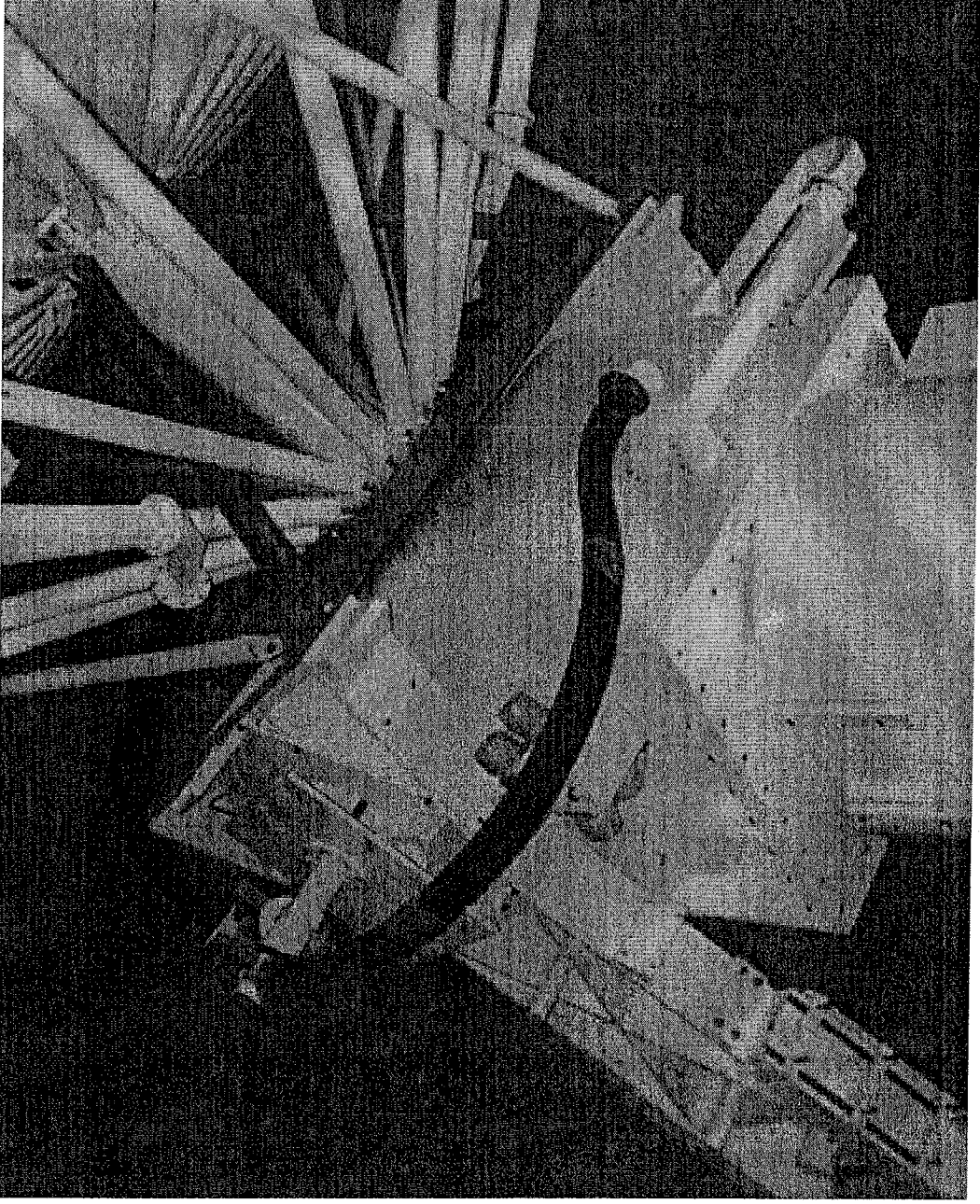
Fig. A1.4 A Photograph of the elevation drive housing. The output of the dual-channel 90°
waveguide assembly is connected to the waveguides which lead to the elevation rotary
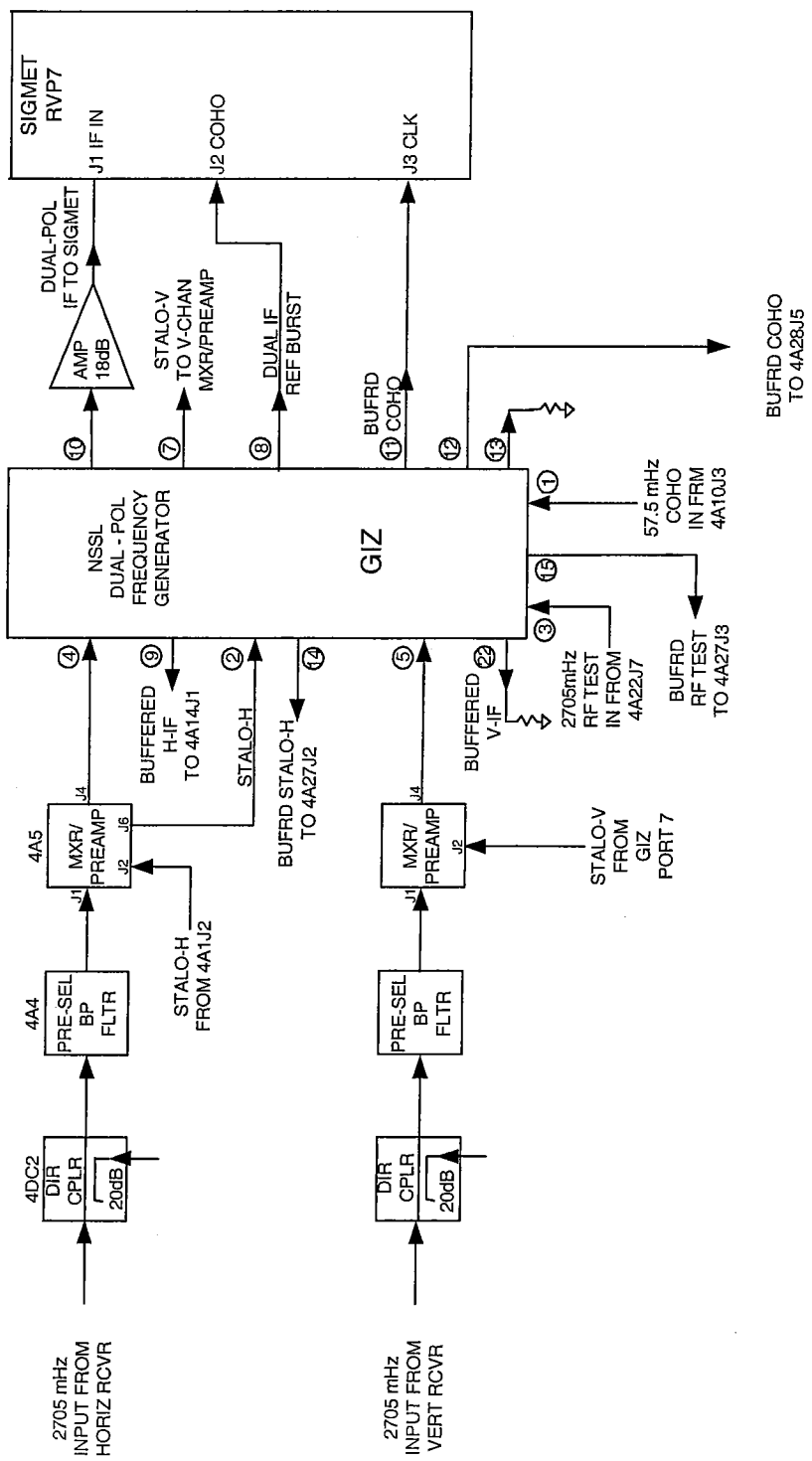joints and then to the waveguide struts supporting the antenna feed shown in Fig. 1.1(b).

Fig. A2.1 A block diagram showing the output connectors of the Dual-Pol Frequency Generator connected to the various circuits of the WSR-88D and the SIGMET processor.
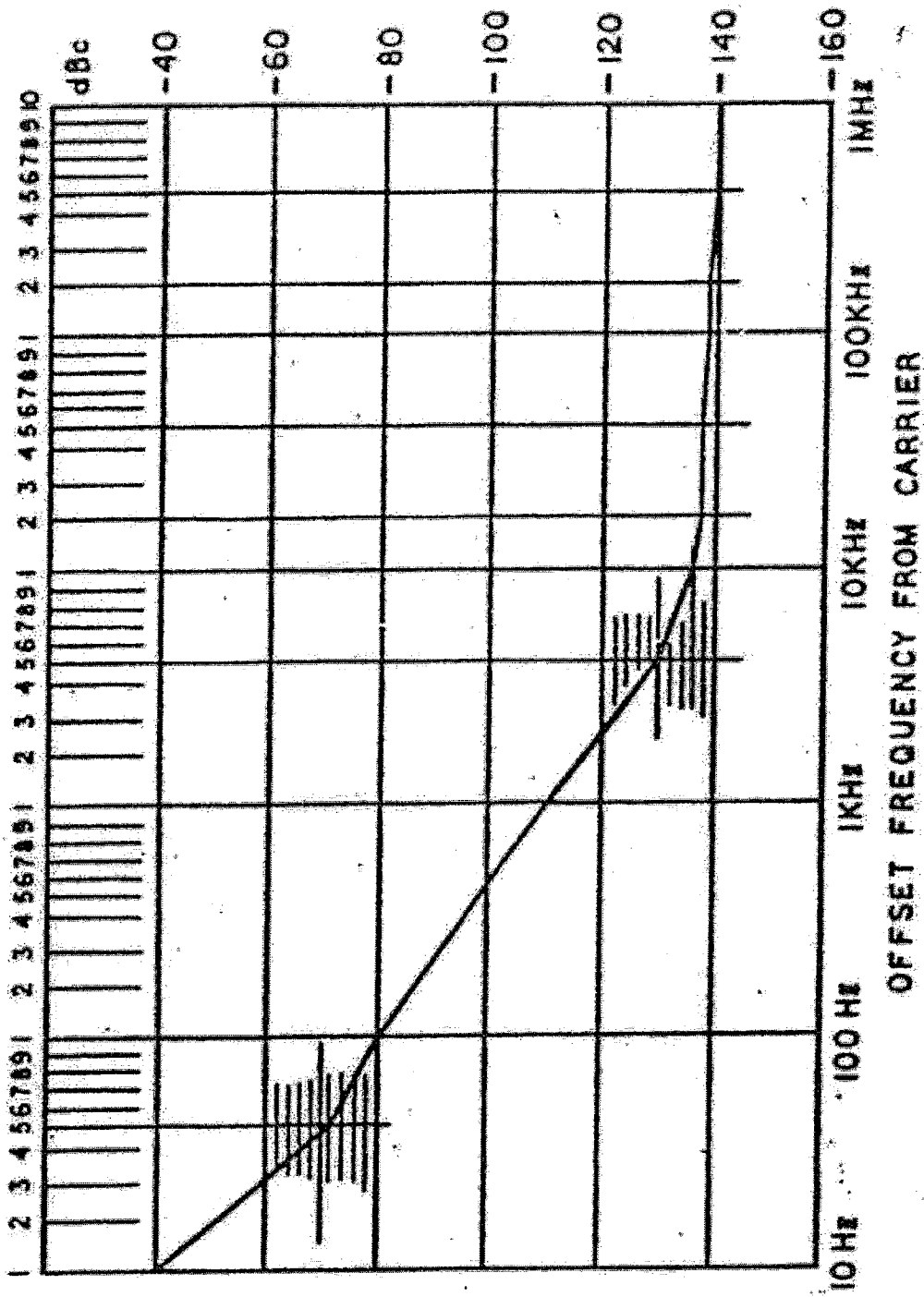
Fig. A2.2 The specifications of the allowable FM noise, in a 1 Hz bandwidth, on the STALOV and the buffered STALOH signals. The dB below the carrier signal power is designated as dBc.
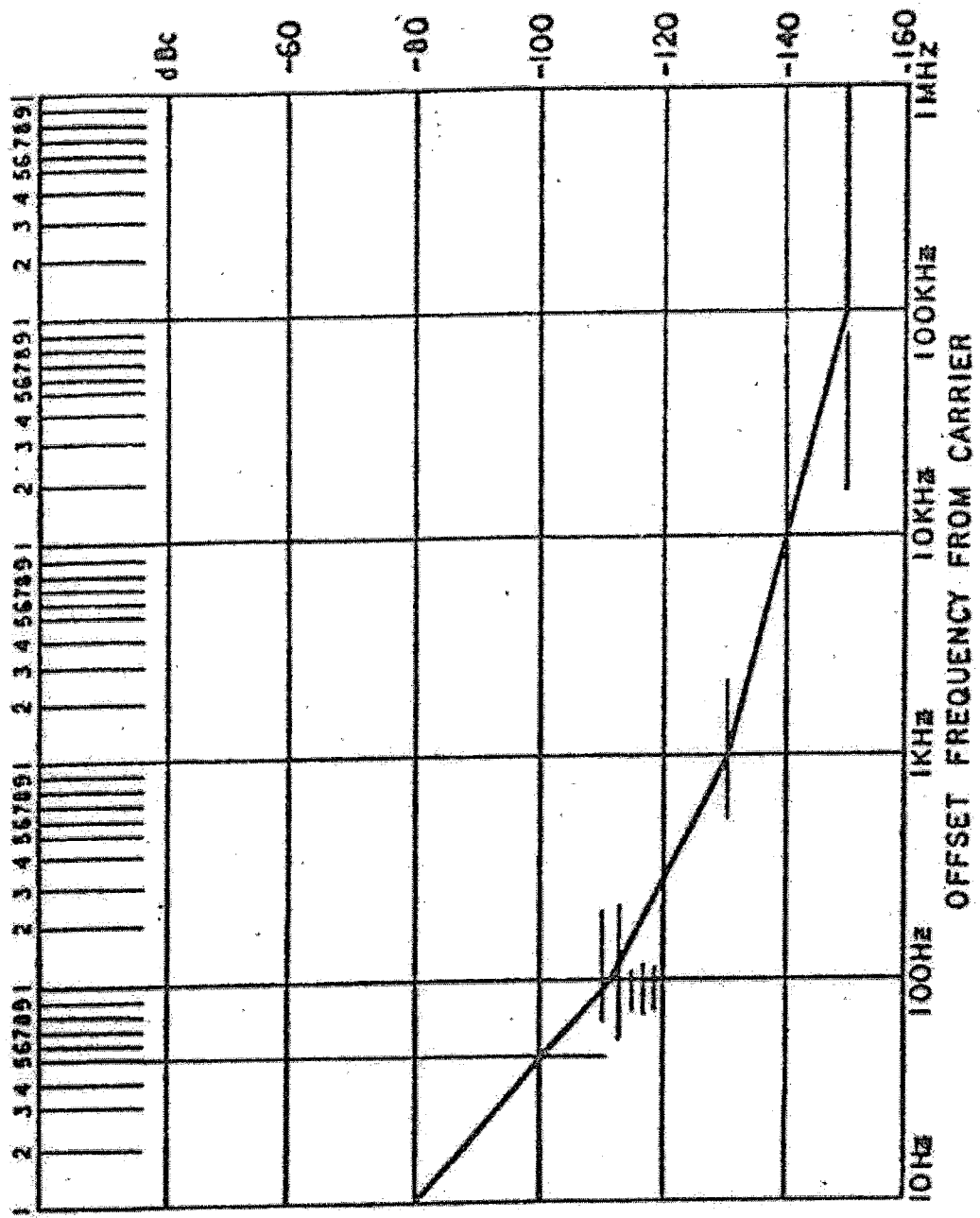
Fig. A2.3 The specifications of the allowable AM noise , in a 1 Hz bandwidth, on the STALOV and the buffered STALOH signals. The dB below carrier power is designated as dBc.